Cord Blood Bank (Hiroshima, Japan). Mononuclear cells (MNCs) from CB samples were isolated using Lymphoprep (Axis-Shield PoC AS, Oslo, Norway) density gradient centrifugation and washed three times in phosphate-buffered saline (PBS). MNCs were then enriched for $CD34^+$ cells using the CD34 Progenitor Cell Selection System (Dynal, Oslo, Norway) according to the manufacturer's instructions. The purity of $CD34^+$ cells (>90%) was determined by flow cytometry.

Cell cultures

Enriched $CD34^+$ cell populations were divided into three aliquots. They were cultured with or without AMD3100 (10 mM; Sigma Chemicals) for 2 h in RPMI-1640 (Sigma Chemicals, St. Louis, MO) without serum at 1×10^6 cells/ml (10^5 to 2×10^5 cells per well) in 96-well round bottom microtiter plates (Costar; Corning, Inc., Corning, NY). All cultures were performed at 37°C under a humidified atmosphere of 5% CO_2. A third aliquot was neither treated nor cultured and used immediately for all experiments without preservation.

Flow cytometric analysis

The presence of cell surface antigens was determined with a FACSCalibur (BD Biosciences, San Jose, CA) using the following fluorescein-conjugated monoclonal antibodies (mAbs): FITC-labeled anti-CD45 (2D1; BD Biosciences), PE-labeled anti-CD34 (AC136; Miltenyi Biotec, Bergisch-Gladbach, Germany), APC-labeled anti-CXCR4 (12G5; BD Biosciences), PE-labeled anti-CD26 (M-A261; BD Biosciences), APC-labeled anti-CD38 (HIT2; BD Biosciences), PE-labeled anti-CD33 (WM53; BD Biosciences), PE-labeled anti-CD19 (SJ25C1; BD Biosciences), and PE-labeled anti-CD3 (UCHT1; BD Biosciences). To identify and disregard dead cells from our analyses, cell cultures were stained with propidium iodide (PI; Sigma Chemicals, St. Louis, MO) at a concentration of 1 μg/mL.

Reverse transcription-polymerase chain reaction (RT-PCR) analysis

RT-PCR was used to determine *CXCR4* mRNA expression in cultured versus noncultured cells. Total RNA from cultured $CD34^+$ cells was extracted using the acid–phenol technique. RT-PCR was performed according to the manufacturer's protocol (Takara Bio, Inc., Shiga, Japan). The following specific primers were used to amplify *CXCR4*: sense, 5'-ggc cct caa gac cac agt ca-3'; antisense, 5'-tta gct gga gtg aaa act tga ag-3' [12]. As an internal control, we also examined the expression of glyceraldehyde-3-phosphate dehydrogenase (*GAPDH*) in all samples. Amplified DNA fragments were then electrophoresed on an agarose gel and visualized by ethidium bromide staining.

Migration assay

Cells were incubated for 30 min at 37°C in 5% CO_2 in the upper chambers of a 96-well transwell apparatus (1×10^5 cells per well; QCM™ Chemotaxis 5 μm 96-Well Cell Migration Assay; Chemicon, Temecula, CA) containing RPMI-1640 medium supplemented with 10% fetal calf serum (FCS; StemCell Technologies, Vancouver, BC, Canada) and then allowed to migrate to the lower chamber containing 125 ng/ml SDF-1α (Sigma Chemicals). The number of cells that migrated to the lower chamber was scored visually with a light microscope.

Transplantation into mice

NOD/Shi-scid jic mice obtained from CLEA (Kawasaki, Japan) were bred and maintained under controlled conditions in individually ventilated (high-efficiency particle-arresting filtered air), sterile microisolator cages at the Hiroshima University Animal Institute. Before transplantation, 6- to 8-week-old mice were subjected to a sublethal dose of 300 cGy total-body irradiation. Then, 1×10^5 cultured or noncultured $CD34^+$ cells were injected into the tail veins of irradiated mice.

Homing assay

Sixteen hours after tail vein injection, the mice were killed and PBS was used to flush bone marrow cells from femurs and tibias. The cells obtained in this manner were analyzed by flow cytometry for the presence of human cells using human-specific anti-CD45-FITC and anti-CD34-PE. At least 1×10^6 cells were analyzed.

Engraftment analysis

To assess the engraftment of human cells into murine bone marrow, cell populations obtained from the murine marrows were incubated with antihuman, fluorescein-conjugated mAbs against CD45, CD34, CD33, CD19, and CD3 and then analyzed via flow cytometry. Engraftment analysis was performed 8 weeks after transplantation.

Secondary transplantation

Bone marrow cells were harvested from NOD/SCID mice in which CB $CD34^+$ cells had previously engrafted. Three mice were injected with 1×10^7 MNCs after sublethal irradiation at 300 cGy. Eight weeks after secondary transplantation, human cells in murine bone marrow were labeled with the same antihuman mAbs used in the primary engraftment analysis and subjected to flow cytometry.

Statistics

All data are expressed as the mean ± standard deviation (SD). Statistically significant differences within the data set were detected using the Student's *t*-test and Wilcoxon's signed-ranks test. All analyses were performed using the StatView software (version 5.0; SAS Institute, Cary, NC).

Results

Flow cytometric analysis of CXCR4 expression on $CD34^+$ cells from umbilical cord blood

Consistent with previous studies, a subpopulation of $CD34^+$ cells from umbilical CB constantly expressed CXCR4 on the cell surface (7.7 ± 3.6%). The cell surface expression of CXCR4 increased after culturing $CD34^+$ cells for 2 h (19.8 ± 8.7, Fig. 1, $P < 0.05$). It increased to >30% after 6 h in culture, but PI staining showed that the nonviable cells at

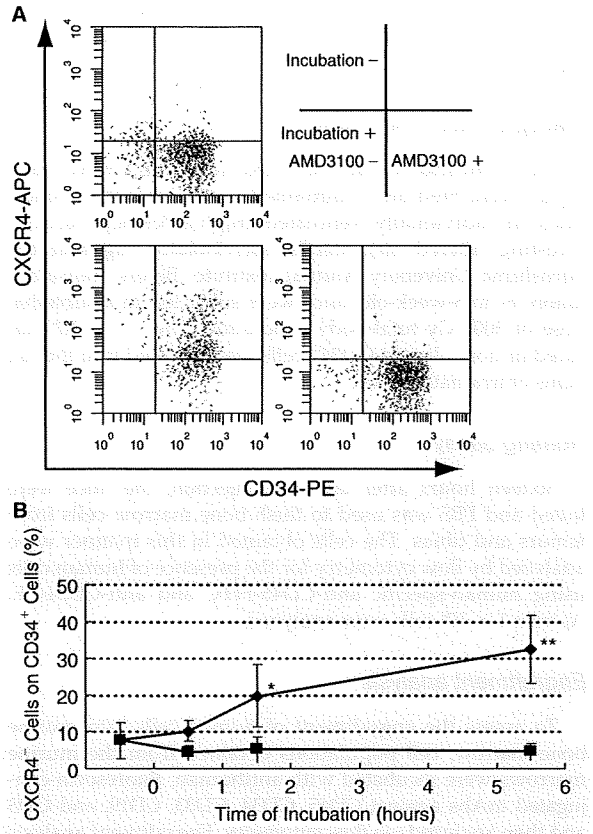

FIG. 1. Effect of short-term culture with or without AMD3100 treatment on CXCR4 expression on $CD34^+$ cells. Representative flow cytometry profiles for CXCR4 expression in cultured cells with or without AMD3100 treatment (**A**). CXCR4 expression on $CD34^+$ cells during short-term incubation with AMD3100 (u) or without AMD3100 (◆) (**B**). Data represent the mean ± SD of six independent experiments. CXCR4 expression increased significantly on the surface of $CD34^+$ cells ($^*P < 0.05$, $^{**}P < 0.01$).

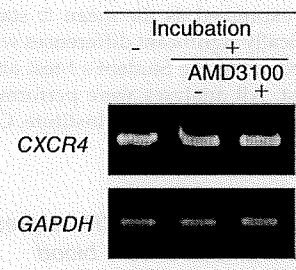

FIG. 2. Effect of short-term incubation on *CXCR4* mRNA expression in $CD34^+$ cells. Total RNA was extracted from cells after the cells were incubated under the indicated culture conditions, RT-PCR was performed. *GAPDH* was used as an internal control. Short-term culture had no effect on *CXCR4* mRNA expression in $CD34^+$ cells.

TABLE 1. PERCENTAGE OF CORD BLOOD $CD34^+$ CELLS THAT ARE $CXCR4^+$, $CD26^+$, AND $CD38^-$

	Incubation		
	(−)	(+)	
Surface markers		*AMD3100*	
		(−)	(+)
$CXCR4^+$	8.0 ± 5.0	19.8 ± 8.7*	5.2 ± 3.4
$CD26^+$	7.7 ± 3.5	7.7 ± 4.7	7.6 ± 3.6
$CD38^+$	4.3 ± 2.0	5.5 ± 3.2	5.3 ± 2.8

Data represent the mean ± SD of six independent experiments. $CD34^+$ cells from Cord Blood were incubated with or without 10 mM AMD3100 for 2 h. $^*P < 0.05$, compared to noncultured and AMD3100-treated cells.

6 h were >30% relative to <10% at 2 h. Viability of the cultured cells at for 2 h was not different from that of the noncultured cells. Culturing for 6 h, therefore, was not done after this first experiment. The increase in the CXCR4 level was not exhibited in the presence of AMD3100, a CXCR4 antagonist. Next, we cultured CD34+ cells in the presence or absence of AMD3100 and examined the expression of CD26, CD38, and CXCR4. As shown in Table 1, a 2-h incubation with AMD3100 did not affect the expression of CD26 or CD38.

RT-PCR analysis of CXCR4 expression

The expression of *CXCR4* mRNA during short-term incubation was examined via RT-PCR. As shown in Figure 2, the addition of AMD3100 had no affect on *CXCR4* mRNA expression after a 2-h incubation. A quantitative real-time RT-PCR analysis using the same samples showed no difference in *CXCR4* expression after a 2-h incubation (data not shown). Thus, the observed increase in cell surface expression was not the result of increased mRNA expression.

Migration and homing activity of cultured cells

Because 2-h incubation increased CXCR4 expression on the surface of $CD34^+$ cells, we examined the in vitro migration of these cells toward the CXCR4 ligand, SDF-1. As shown in Figure 3, over 25% of $CD34^+$ cells cultured for 2 h showed transmigration in response to SDF-1. However, transmigrational activity was significantly lower in noncultured cells and in cells which had been cultured in the presence of AMD3100 ($P < 0.05$). Furthermore, the effect of increased CXCR4 expression on homing activity was determined by evaluating the presence of human CD45+/CD34+ cells in mouse bone marrow 16 h after tail vein injection. As shown in Figure 4A, a cluster of CD45+/CD34+ cells (R1) was detected in the bone marrow of mice injected with cultured CD34+ cells. Homing activity was compared among cells cultured in the presence and absence of AMD3100 and noncultured cells. Cultured CD34+ cells demonstrated significantly greater homing activity compared to noncultured cells and to cells cultured in the presence of AMD3100 ($P < 0.05$ in each case).

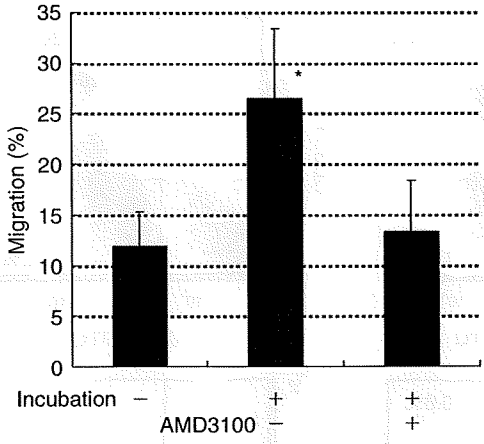

FIG. 3. Effect of short-term incubation and AMD3100 treatment on transmigrational activity in $CD34^+$ cells. $CD34^+$ cells were loaded into the upper wells of a transwell apparatus and incubated for 2 h. Migration was assessed according to the percentage of cells migrated to lower wells containing SDF-1. The data represent the mean ± SD of six independent experiments. $*P < 0.05$, significant increase compared to noncultured and AMD3100-treated cells.

Engraftment of cultured $CD34^+$ cells into NOD/SCID mice

Figure 5 shows a representative FACS analysis of human marrow cells in bone marrow from identical NOD/SCID mice after $CD34^+$ cell transplantation. The presence of human cells was detected by the cell surface expression of CD45, CD34, CD33, CD19, and CD3. The recipients exhibited $CD45^+/CD19^+$ B-lymphoid cells, $CD45^+/CD33^+$ granulomonopoietic cells, and $CD45^+/CD34^+$ immature cells, but not $CD3^+$ T cells. The percentage of $CD34^+/CD19^+$ positive cells in the $CD45^+$ cells was 6–12%, consistent with the report of Kobari et al. [13]. Next, at 8 weeks, we performed a secondary transplant of engrafted cells from previously transplanted mice to determine if long-term engraftment of self-renewing cultured CB cells had occurred. Successful secondary engraftment occurred as shown by the presence of $CD45^+/CD19^+$ cells and possibly $CD45^+/CD34^+$ cells (Fig. 5B).

To assess the effect of short-term culture and AMD3100 interference on engraftment, $CD34^+$ cells were cultured with or without AMD3100 as indicated and injected into NOD/SCID mice via the tail vein. Eight weeks after transplantation, engraftment was assessed based on the expression of the human CD45 antigen. As shown in Figure 6, cultured $CD34^+$ cells showed increased engraftment into murine bone marrow compared to noncultured $CD34^+$ cells (32.0 ± 21.4% vs. 17.1 ± 15.7%), $P < 0.01$, or to $CD34^+$ cells from AMD3100-treated cultures (12.9 ± 11.1%), $P < 0.01$, as determined by Wilcoxon's signed-ranks test.

Discussion

Umbilical CB contains hematopoietic cells capable of engrafting into NOD/SCID mice in vivo. Our results demonstrate that short-term culture in the absence of serum and/or cytokines induced the expression of CXCR4 on umbilical

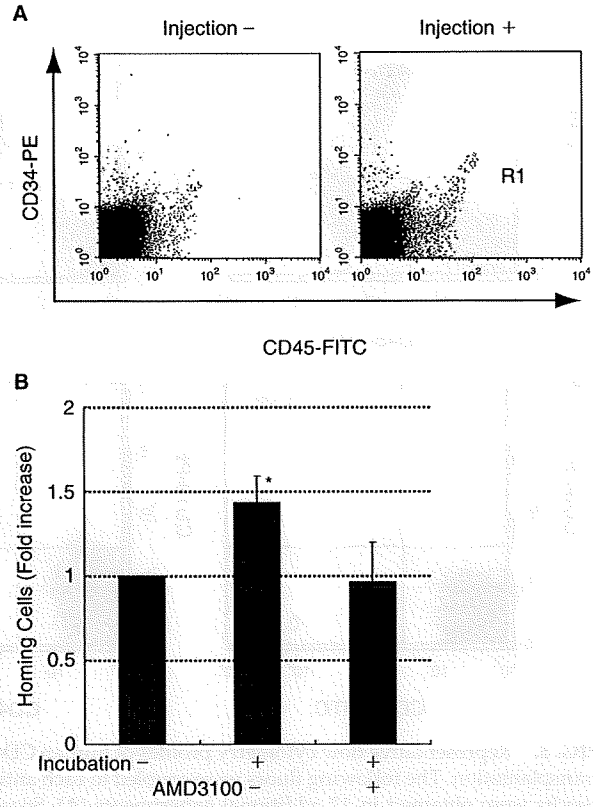

FIG. 4. Homing activity of $CD34^+$ cells in NOD/SCID mice. $CD34^+$ cells were cultured as indicated and then injected into the tail veins of NOD/SCID mice. After 16 h, the mice were killed and human-derived cells in the bone marrow were quantified based on the presence of a $CD45^+/CD34^+$ cluster (R1) in flow cytometry (**A**). The fold-increase compared to noninjected mice was calculated (**B**). The data represent the mean ± SD of six independent experiments. $*P < 0.05$, significant increase compared to noncultured and AMD3100-treated cells.

CB-derived $CD34^+$ cells, resulting in enhanced homing activity and subsequently improved engraftment into NOD/SCID mice. The enhanced homing and engraftment of short-term cultured CD34+ cells was abolished by the addition of AMD3100 to the cultures, suggesting that improved engraftment was dependent upon increased CXCR4 expression.

Lataillade et al. [14] reported that cell surface expression of CXCR4 increased significantly when purified progenitor cells were incubated overnight in serum. Peled et al. [9] demonstrated that human $CD34^+$ cells incubated with stem cell factor and IL-6 for 48 h showed increased CXCR4 expression, resulting in enhanced in vitro migration toward an SDF-1 gradient and increased homing and repopulating potential in NOD/SCID and NOD/SCID/beta2-microglobulin null mice. In contrast, the long-term culture of $CD34^+$ cells in a cytokine cocktail decreased CXCR4 expression and led to reduced repopulating potential in immunodeficient mice [15]. The mechanism underlying CXCR4 up-regulation during incubation remains unclear, although various factors, including cell surface adhesion molecules, cell–cell

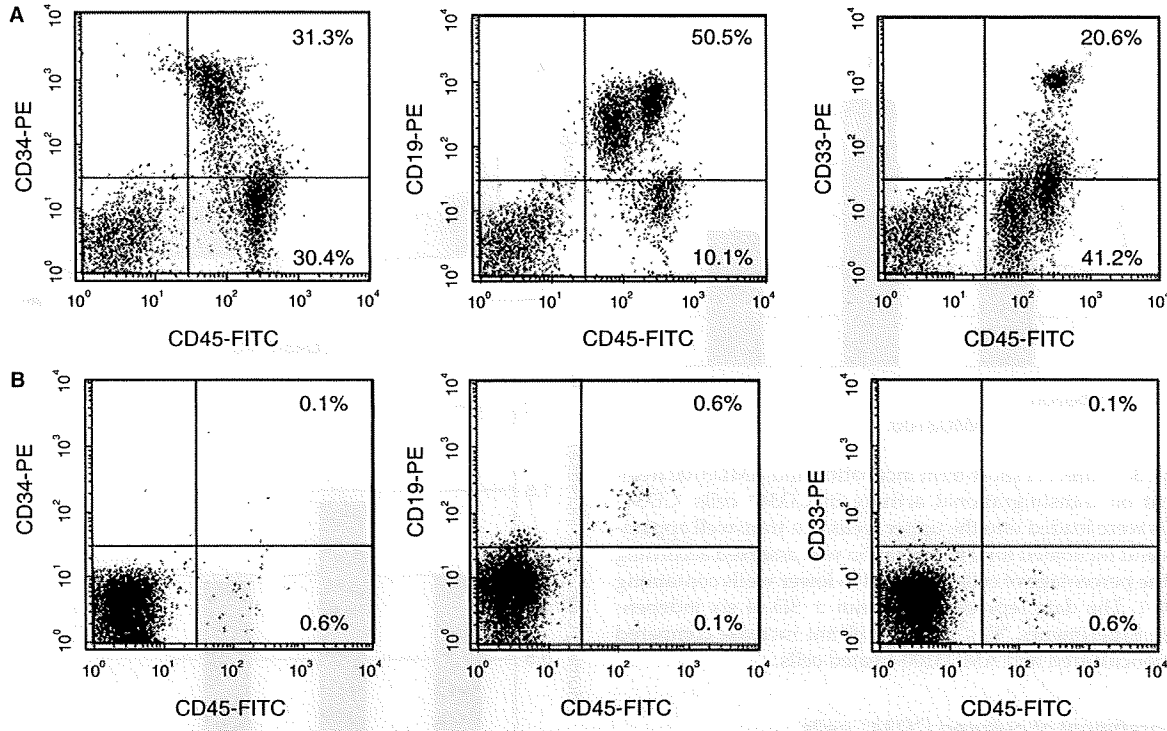

FIG. 5. Representative flow cytometry profiles of human CD45$^+$, CD34$^+$, CD33$^+$, and CD19$^+$ cells obtained at 8 weeks after transplantation. The following fluors were coupled to each antibody: CD45-FITC, CD34-PE, CD33-PE, and CD19-PE. Similar results were obtained in 12 additional experiments (**A**). Secondary transplantation of bone marrow cells obtained from previously transplanted mice (**B**). Marrow cells obtained at 8 weeks.

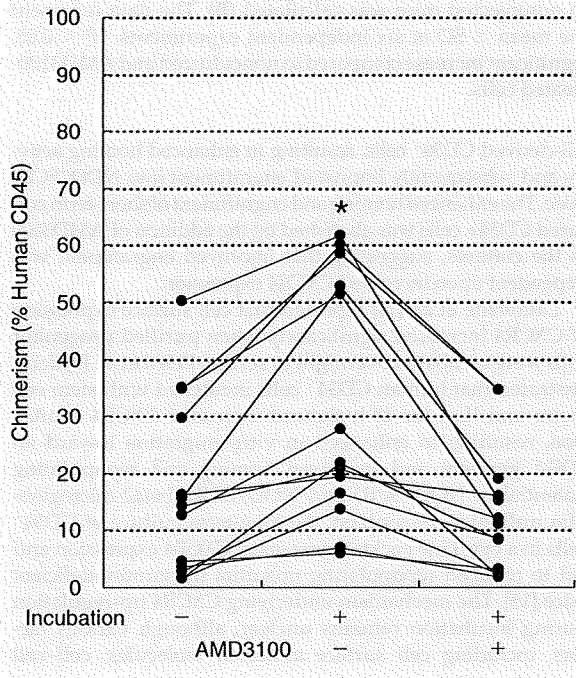

FIG. 6. Engraftment of CD34$^+$ cells with or without the presence of AMD3100 into NOD/SCID mice. CD34$^+$ cells were cultured as indicated and then injected into the tail veins of NOD/SCID mice. Eight weeks after transplantation, the mice were killed and percentage of human CD45$^+$ cells was determined. The data represent the percentage of human CD45$^+$ cells in 13 independent experiments. Statistically significant differences among cultured, noncultured, and AMD3100-treated cells were analyzed using Wilcoxon's signed-ranks test. *$P < 0.01$, significant increase compared to noncultured and AMD3100-treated cells.

contact between $CD34^+$ and low-density MNCs, growth factor production, and adhesion molecule interactions, may be involved [4,5,16]. Our RT-PCR results showed that cell surface CXCR4 expression increased in cultured $CD34^+$ cells without concomitant increases in mRNA expression.

CXCR4 is thought to play a crucial role in the homing and retention of HSCs in murine bone marrow [9] and is required for the retention of B-lineage and myeloid precursors in the bone marrow [16]. Recently, Kahn et al. [11] reported that the overexpression of CXCR4 in human $CD34^+$ cells via gene transfer increased proliferation, migration, and NOD/SCID repopulation. Similarly, we confirmed the importance of CXCR4 expression in $CD34^+$ cell in NOD/SCID marrow homing through the inhibitory effect of AMD3100. AMD3100, a small bicyclam molecule, reversibly inhibits SDF-1–CXCR4 binding [17].

Conclusion

In conclusion, we demonstrated that short-term culture of CB-derived $CD34^+$ cells increased CXCR4 expression on these cells, resulting in increases in in vivo homing and engraftment into NOD/SCID mice. Thus, short-term culture of hematopoietic stem/progenitor cells in the absence of sera and cytokines may serve as a simple but effective way to enhance their repopulating activity.

Acknowledgments

This study was supported in part by a grant (to M.K.) from the Ministry of Education, Culture, Sports, Science, and Technology, Japan and by a grant from the Ministry of Health, Labour, and Welfare, Japan. We thank Chugoku-Shikoku Regional Cord Blood Bank for providing umbilical cord blood used in this study and Animal facility in Hiroshima University for help in breeding the immunodeficient mice. We also thank the Analysis Center of Life Science, Hiroshima University and the division of blood transfusion service of Hiroshima University Hospital for providing the technical assistance.

Author Disclosure Statement

There is no possible conflict of interest (including financial and other relationship) for each author.

References

1. American Academy of Pediatrics Section on Hematology/Oncology; American Academy of Pediatrics Section on Allergy/Immunology, Lubin BH and WT Shearer. (2007). Cord blood banking for potential future transplantation. Pediatrics 119:165–170.
2. McCune JM, R Namikawa, H Kaneshima, LD Shultz, M Lieberman and IL Weissman. (1988). The SCID-hu mouse: murine model for the analysis of human hematolymphoid differentiation and function. Science 241:1632–1639.
3. Mosier DE, RJ Gulizia, SM Baird and DB Wilson. (1988). Transfer of a functional human immune system to mice with severe combined immunodeficiency. Nature 335:256–259.
4. Roland J, BJ Murphy, B Ahr, V Robert-Hebmann, V Delauzun, KE Nye, C Devaux and M Biard-Piechaczyk. (2003). Role of the intracellular domains of CXCR4 in SDF-1-mediated signaling. Blood 101:399–406.
5. Martin C, PC Burdon, G Bridger, JC Gutierrez-Ramos, TJ Williams and SM Rankin. (2003). Chemokines acting via CXCR2 and CXCR4 control the release of neutrophils from the bone marrow and their return following senescence. Immunity 19:583–593.
6. Suratt BT, JM Petty, SK Young, KC Malcolm, JG Lieber, JA Nick, JA Gonzalo, PM Henson and GS Worthen. (2004). Role of the CXCR4/SDF-1 chemokine axis in circulating neutrophil homeostasis. Blood 104:565–571.
7. Semerad CL, F Liu, AD Gregory, K Stumpf and DC Link. (2002). G-CSF is an essential regulator of neutrophil trafficking from the bone marrow to the blood. Immunity 17, 413–423.
8. Lapidot T and O Kollet. (2002). The essential roles of the chemokine SDF-1 and its receptor CXCR4 in human stem cell homing and repopulation of transplanted immune-deficient NOD/SCID and NOD/SCID/B2m (null) mice. Leukemia 16:1992–2003.
9. Peled A, I Petit, O Kollet, M Magid, T Ponomaryov, T Byk, A Nagler, H Ben-Hur, A Many, L Shultz, O Lider, R Alon, D Zipori and T Lapidot. (1999). Dependence of human stem cell engraftment and repopulation of NOD/SCID mice on CXCR4. Science 283:845–848.
10. Kollet O, I Petit, J Kahn, S Samira, A Dar, A Peled, V Deutsch, M Gunetti, W Piacibello, A Nagler and T Lapidot. (2002). Human CD34(+) CXCR4(-) sorted cells harbor intracellular CXCR4, which can be functionally expressed and provide NOD/SCID repopulation. Blood 100:2778–2786.
11. Kahn J, T Byk, L Jansson-Sjostrand, I Petit, S Shivtiel, A Nagler, I Hardan, V Deutsch, Z Gazit, D Gazit, S Karlsson and T Lapidot. (2004). Overexpression of CXCR4 on human CD34+ progenitors increases their proliferation, migration, and NOD/SCID repopulation. Blood 103:2942–2949.
12. Bajetto A, R Bonavia, S Barbero, P Piccioli, A Costa, T Florio and G Schettini. (1999). Glial and neuronal cells express functional chemokine receptor CXCR4 and its natural ligand stromal cell-derived factor 1. J Neurochem 73:2348–2357.
13. Kobari L, F Pflumio, M Giarratana, X Li, M Titeux, B Izac, F Leteurtre, L Coulombel and L Douay. (2000). In vitro and in vivo evidence for the long-term multilineage (myeloid, B, NK, and T) reconstitution capacity of ex vivo expanded human CD34(+) cord blood cells. Exp Hematol 28:1470–1480.
14. Lataillade JJ, D Clay, C Dupuy, S Rigal, C Jasmin, P Bourin and MC Le Bousse-Kerdilès. (2000). Chemokine SDF-1 enhances circulating CD34(+) cell proliferation in synergy with cytokines: possible role in progenitor survival. Blood 95:56–768.
15. Denning-Kendall P, S Singha, B Bradley and J Hows. (2003). Cytokine expansion culture of cord blood $CD34^+$ cells induces marked and sustained changes in adhesion receptor and CXCR4 expressions. Stem Cells 21:61–70.
16. Herrera C, J Sanchez, A Torres, A Pascual, A Rueda and MA Alvarez. (2004). Pattern of expression of CXCR4 and adhesion molecules by human $CD34^+$ cells from different sources: role in homing efficiency in NOD/SCID mice. Haematologica 89:1037–1045.
17. Ma Q, D Jones and TA Springer. (1999). The chemokine receptor CXCR4 is required for the retention of B lineage and granulocytic precursors within the bone marrow microenvironment. Immunity 10:463–471.

Address correspondence to:
Dr. Masao Kobayashi
Department of Pediatrics
Hiroshima University Graduate School of Biomedical Sciences
1-2-3, Kasumi, Minami-ku
Hiroshima 734-8551
Japan

E-mail: masak@hiroshima-u.ac.jp

Received for publication October 6, 2008
Accepted after revision December 29, 2008
Prepublished on Liebert Instant Online December 29, 2008

THE JOURNAL OF BIOLOGICAL CHEMISTRY VOL. 284, NO. 13, pp. 8548–8556, March 27, 2009

FBP17 Mediates a Common Molecular Step in the Formation of Podosomes and Phagocytic Cups in Macrophages*[S]

Received for publication, July 23, 2008, and in revised form, December 29, 2008 Published, JBC Papers in Press, January 20, 2009, DOI 10.1074/jbc.M805638200

Shigeru Tsuboi[‡1], Hidetoshi Takada[§], Toshiro Hara[§], Naoki Mochizuki[¶], Tomihisa Funyu[‖], Hisao Saitoh[‖], Yuriko Terayama[‖], Kanemitsu Yamaya[‖], Chikara Ohyama[**], Shigeaki Nonoyama[‡‡], and Hans D. Ochs[§§]

From the [‡]Infectious and Inflammatory Disease Center, Burnham Institute for Medical Research, La Jolla, California 92037, the [§]Department of Pediatrics, Graduate School of Medical Sciences, Kyushu University, Fukuoka 812-8582, Japan, the [¶]Department of Structural Analysis, National Cardiovascular Center Research Institute, Osaka 565-8565, Japan, the [‖]Oyokyo Kidney Research Institute, Hirosaki 036-8243, Japan, the [**]Department of Urology, Hirosaki University School of Medicine, Hirosaki 036-8562, Japan, the [‡‡]Department of Pediatrics, National Defense Medical College, Saitama 359-0042, Japan, and the [§§]Department of Pediatrics, Research Center for Immunity and Immunotherapy, Seattle Children's Hospital Research Institute, Seattle, Washington 98101

Macrophages act to protect the body against inflammation and infection by engaging in chemotaxis and phagocytosis. In chemotaxis, macrophages use an actin-based membrane structure, the podosome, to migrate to inflamed tissues. In phagocytosis, macrophages form another type of actin-based membrane structure, the phagocytic cup, to ingest foreign materials such as bacteria. The formation of these membrane structures is severely affected in macrophages from patients with Wiskott-Aldrich syndrome (WAS), an X chromosome-linked immunodeficiency disorder. WAS patients lack WAS protein (WASP), suggesting that WASP is required for the formation of podosomes and phagocytic cups. Here we have demonstrated that formin-binding protein 17 (FBP17) recruits WASP, WASP-interacting protein (WIP), and dynamin-2 to the plasma membrane and that this recruitment is necessary for the formation of podosomes and phagocytic cups. The N-terminal EFC (extended FER-CIP4 homology)/F-BAR (FER-CIP4 homology and Bin-amphiphysin-Rvs) domain of FBP17 was previously shown to have membrane binding and deformation activities. Our results suggest that FBP17 facilitates membrane deformation and actin polymerization to occur simultaneously at the same membrane sites, which mediates a common molecular step in the formation of podosomes and phagocytic cups. These results provide a potential mechanism underlying the recurrent infections in WAS patients.

Podosomes (see Fig. 1*A*) are micron-scale, dynamic, actin-based protrusions observed in motile cells such as macrophages, dendritic cells, osteoclasts, certain transformed fibroblasts, and carcinoma cells (1). Podosomes play an important role in macrophage chemotactic migration, which is critical for recruitment of leukocytes to inflamed tissues. Podosomes are both adhesion structures and the sites of extracellular matrix degradation (2). Adhesion to and degradation of the extracellular matrix are essential processes for the successful migration of macrophages in tissues. Podosomes occur in most macrophages and can be observed by differentiating human primary monocytes into macrophages with macrophage-colony stimulating factor-1 (M-CSF-1)[2] and staining the F-actin using phalloidin (3, 4). Podosomes labeled in this way appear as F-actin-rich dots (see Fig. 1*C*). Podosome formation has recently been directly observed *in vitro* and *in vivo* in leukocyte migration through the endothelium, diapedesis (5).

Phagocytosis of bacterial pathogens is one of the most important primary host defense mechanisms against infections. The phagocytic cup (see Fig. 1*B*) is an actin-based membrane structure formed at the plasma membrane of phagocytes, including macrophages, upon stimulation with foreign materials such as bacteria. The phagocytic cup captures and ingests foreign materials, and its formation is an essential first step in phagocytosis leading to the digestion of foreign materials (6, 7). When macrophages are stimulated by foreign materials, podosomes disappear, and phagocytic cups, which are also rich in F-actin, are formed to ingest the foreign materials (see Fig. 1*D*).

Wiskott-Aldrich syndrome (WAS) is an X chromosome-linked immunodeficiency disorder. Patients with WAS suffer from severe bleeding, eczema, recurrent infection, autoimmune diseases, and an increased risk of lymphoreticular malignancy (8–10). The causative gene underlying WAS encodes Wiskott-Aldrich syndrome protein (WASP) (11). WASP deficiency due to the mutation or deletion causes defects in adhesion, chemotaxis, phagocytosis, and the development of hematopoietic cells in WAS patients (10).

* This work was supported, in whole or in part, by National Institutes of Health Grant R01HD042752 (to S. T.). The costs of publication of this article were defrayed in part by the payment of page charges. This article must therefore be hereby marked "*advertisement*" in accordance with 18 U.S.C. Section 1734 solely to indicate this fact.

[S] The on-line version of this article (available at http://www.jbc.org) contains six supplemental figures.

[1] To whom correspondence should be addressed: Dept. of Biochemistry, Oyokyo Kidney Research Institute, 90 Yamazaki, Kozawa, Hirosaki 036-8243, Japan. Tel.: 81-172-87-1221; Fax: 81-172-87-1228; E-mail: tsuboi@oyokyo.jp.

[2] The abbreviations used are: M-CSF-1, macrophage-colony stimulating factor-1; FBP17, formin-binding protein 17; WAS, Wiskott-Aldrich syndrome; WASP, Wiskott-Aldrich syndrome protein; N-WASP, neuronal WASP; WIP, WASP interacting-protein; EFC domain, extended FER-CIP4 homology domain; F-BAR domain, FER-CIP4 homology and Bin-amphiphysin-Rvs domain; PMA, phorbol 12-myristate 13-acetate; GFP, green fluorescence protein; siRNA, short interfering RNA; FITC, fluorescein isothiocyanate; PDZ-GEF, PDZ-guanine nucleotide exchange factor; HEK293 cells, human embryonic kidney 293 cells; HA, hemagglutinin; SH3, src homology 3 domain; dSH3, SH3 domain deletion; GST, glutathione *S*-transferase; , $PI(4,5)P_2$, phosphatidylinositol 4,5-bisphosphate; siFBP, siRNA for FBP17; siC, scrambled control siRNA.

The formation of podosomes and phagocytic cups is severely affected in macrophages from WAS patients (3, 12, 42), suggesting that WASP is involved in the formation of these structures. However, the detailed molecular mechanisms of their formation remain unknown. WASP is complexed with a cellular WASP-interacting partner, WASP-interacting protein (WIP) (13, 14). Recently, two groups (including us) have demonstrated that WASP and WIP form a complex and that the WASP-WIP complex is required for the formation of podosomes (4, 15) and phagocytic cups (16). Here, we identified formin-binding protein 17 (FBP17) as a protein interacting with the WASP-WIP complex and examined the role of FBP17 in the formation of podosomes and phagocytic cups.

EXPERIMENTAL PROCEDURES

Reagents and Antibodies—Recombinant human macrophage-colony stimulating factor-1 (M-CSF-1) was purchased from R&D Systems (Minneapolis, MN). Phenylmethylsulfonyl fluoride, leupeptin, pepstain A, aprotinin, IGEPAL CA-630, paraformaldehyde, saponin, bovine serum albumin, 3-methyladenine, latex beads (3 μm in diameter), phorbol 12-myristate 13-acetate (PMA), human IgG, glycerol, Triton X-100, anti-FLAG monoclonal antibody (M2), and anti-β-actin antibody were purchased from Sigma-Aldrich. The anti-WASP monoclonal antibody, anti-WIP polyclonal antibody, and anti-Myc monoclonal antibody (9E10) were obtained from Santa Cruz Biotechnology Inc. (Santa Cruz, CA). The anti-dynamin-2 antibody was purchased from BD Biosciences. The rat anti-hemagglutinin (HA) monoclonal antibody (3F10) was purchased from Boehringer Ingelheim (Ridgefield, CT). The Cy2-labeled anti-rat IgG was obtained from Jackson ImmunoResearch Laboratories (West Grove, PA).

Yeast Two-hybrid Screening—We screened a human lymphocyte cDNA library (Origene Technology Inc., Rockville, MD) using a full-length WIP as bait. A cDNA encoding full-length WIP was cloned into pGilda (BD Biosciences Clontech). The EGY48 yeast strain was transformed with pGilda-WIP, the human lymphocyte cDNA library, and pSH18–34, a reporter plasmid for the β-galactosidase assay. Transformants were assayed for Leu prototrophy, and a filter assay was performed for β-galactosidase measurement (17).

Cells and Transfection—THP-1 and human embryonic kidney (HEK) 293 cells were purchased from the American Type Culture Collection (Manassas, VA) and cultured in RPMI1640 and Dulbecco's modified Eagle's high glucose medium (Invitrogen), respectively, both supplemented with 10% fetal bovine serum. For human primary monocyte isolation, 10–30 ml of peripheral blood was drawn from healthy volunteers and WAS patients after informed consent was obtained. Monocytes were prepared from peripheral blood samples (10–30 ml) using a monocyte isolation kit II (Miltenyi Biotech Inc., Auburn, CA). Transfection of THP-1 cells and monocytes was performed with a Nucleofector device using a cell line Nucleofector kit V and a human monocyte Nucleofector kit, respectively, according to the manufacturer's instructions (Amaxa Biosystems, Gaithersburg, MD). Transfection of HEK293 cells was performed using SuperFect transfection reagent (Qiagen, Valencia, CA). THP-1 cells and monocytes were co-transfected with the FBP17 constructs and a GFP-expressing plasmid, pmaxGFP (Amaxa Biosystems Inc.), as a transfection marker. The transfection efficiency measured using pmaxGFP was 40–50% for THP-1 cells and 10–20% for monocytes.

RNA Interference—A short interfering RNA (siRNA) for FBP17 and its scrambled control siRNA was synthesized by Dharmacon (Lafayette, CO). The targeting sequence was 5′-CCCACTTCATATGTCGAAGTCTGTT-3′ (18). THP-1 cells and monocytes were transfected with siRNA using a cell line Nucleofector kit V and a human monocyte Nucleofector kit, respectively, and a Nucleofector device. Cells were co-transfected with an fluorescein isothiocyanate (FITC)-conjugated control siRNA, BLOCK-IT (Invitrogen), as a transfection marker. The transfection efficiency measured using BLOCK-IT was 40–50% for THP-1 cells and 10–20% for monocytes.

Immunoprecipitation—For immunoprecipitation of WASP from THP-1 cells, 2×10^7 cells were lysed in buffer A (50 mM Tris-HCl, pH 7.5, 75 mM NaCl, 1% Triton X-100, 1 mM phenylmethylsulfonyl fluoride, 1 μg/ml leupeptin, 1 μg/ml pepstatin A, 1 μg/ml aprotinin). Lysates were centrifuged at 10,000 $\times g$ at 4 °C for 15 min. The supernatant was incubated with 2 μg/ml anti-WASP monoclonal antibody (Santa Cruz Biotechnology) at 4 °C for 2 h and then incubated with anti-mouse IgG agarose (Sigma). The resin binding the immune complex was washed three times with 0.5 ml of buffer B (50 mM Tris-HCl, pH 7.5, 10% glycerol, 0.1% Triton X-100), and the complex was eluted with 1× Laemmli's SDS-PAGE sample buffer. Eluted proteins were subjected to SDS-PAGE and analyzed by immunoblotting for WASP, WIP, and FBP17.

GST Pull-down Assay—Glutathione *S*-transferase (GST) and a fusion protein of GST and the src homology 3 (SH3) domain of FBP17 (548–609 amino acids) (GST-FSH3) were purified from *Escherichia coli* (XL-1B) extracts using glutathione-Sepharose-4B. HEK293 cells were transfected with the cDNAs of Myc- or FLAG-tagged protein and lysed in buffer A. Lysates from the transfected cells were incubated with the affinity matrices of GST alone or GST-FSH3 at 4 °C for 1 h. After a 1-h incubation, the matrices were washed five times with buffer A, and pull-down samples were analyzed by immunoblotting using anti-Myc or anti-FLAG antibody.

Immunofluorescence Microscopy—THP-1 cells and monocytes grown on coverslips were differentiated into macrophages by incubation with 12.5 ng/ml PMA (Sigma) and 20 ng/ml M-CSF-1 (R&D Systems), respectively, for 72 h. HEK293 cells were transfected with various cDNA constructs and then cultured on coverslips for 48 h. Cells were fixed with 4% (w/v) paraformaldehyde, permeabilized with 0.1% (w/v) saponin, and blocked with 1% (w/v) bovine serum albumin. Cells were stained with primary antibodies and Alexa Fluor 488- or Alexa Fluor 564-labeled secondary antibodies (Invitrogen). Cells were also stained with Alexa Fluor 568-labeled phalloidin (Invitrogen). Cell staining was examined under a fluorescence microscope (Zeiss Axioplan AR) or an MRC 1024 SP laser point scanning confocal microscope (Bio-Rad).

Assays for the Formation of Podosomes and Phagocytic Cups—The formation of podosomes and phagocytic cups was assayed by visualizing these actin-based membrane structures by F-actin staining as described previously (4, 16). Briefly, podosomes

in differentiated THP-1 cells or macrophages were visualized by F-actin staining with Alexa Fluor 568-phalloidin. To form phagocytic cups in differentiated THP-1 cells or macrophages, latex beads (3 μm, Sigma) were opsonized with 0.5 mg/ml human IgG (Sigma), and cells grown on coverslips were incubated with the IgG-opsonized latex beads at 37 °C for 10 min in the presence of 10 mM 3-methyladenine (Sigma) to stabilize the phagocytic cups (16). The phagocytic cups were then also visualized with Alexa Fluor 568-phalloidin. Cells were examined under a fluorescence microscope (Zeiss Axioplan AR).

Assays for Macrophage Migration and Phagocytosis—For the macrophage migration assay, human macrophages (2×10^5 cells) were plated onto chemotaxis membranes with 5-μm pores (Corning, Acton, MA) coated with 0.15% gelatin/phosphate-buffered saline placed within Boyden chamber inserts. M-CSF-1 was used as a chemoattractant and diluted in serum-containing RPMI 1640 medium in lower chambers. After a 4-h incubation, non-migrating cells were removed by gently wiping the upper surface of the filter. The filter was removed from the inserts using a razor blade and mounted onto glass plates, and the number of migrating cells was counted under a fluorescence microscope. For the phagocytosis assay, human macrophages (1×10^6 cells) were seeded on coverslips and incubated with 0.5 ml of RPMI 1640 medium containing IgG-opsonized latex beads (3 μm) at 4 °C for 10 min, allowing the beads to attach to cells. Phagocytosis was initiated by adding 1.5 ml of preheated RPMI 1640 medium, and the cells were incubated with the beads at 37 °C for 30 min. Control plates were incubated at 4 °C to estimate nonspecific binding of latex beads to the cells. After incubation, the cells were vigorously washed with phosphate-buffered saline, and the number of intracellular latex beads was determined by counting beads within cells under a fluorescence microscope. The percentage of phagocytosis was calculated as the total number of cells with at least one bead as a percentage of the total number of cells counted. At least 100 cells were examined.

Cell Fractionation—To prepare the cytoplasmic and membrane fractions, macrophages (1×10^6 cells) were washed with ice-cold phosphate-buffered saline and suspended in 50 mM Tris-HCl buffer, pH 7.5, containing 1 mM EDTA and proteinase inhibitors as described above. The cell suspensions were sonicated four times on ice for 5 s each using a bath-type sonicator followed by ultracentrifugation at 265,000 × *g* at 4 °C for 2 h. The supernatant was used as the cytosolic fraction, and the pellet was resuspended in 50 mM Tris-HCl, pH 7.5, containing 1 mM EDTA and used as the membrane fraction. Anti-Caspase-3 (Santa Cruz Biotechnology) and anti-sodium potassium ATPase antibodies (AbCam, Inc., Cambridge, MA) were used to determine the purity of the cytosolic and membrane fractions, respectively.

Statistics—Statistically significant differences were determined using the Student's *t* test. Differences were considered significant if $p < 0.05$.

RESULTS

FBP17 Binds to the WASP-WIP Complex and Dynamin-2 in Macrophages—To explore the detailed molecular mechanisms of the formation of podosomes and phagocytic cups, we searched for a protein interacting with the WASP-WIP complex. We identified FBP17 as a WIP-binding protein in a yeast two-hybrid screen using the full-length WIP as bait. FBP17 was originally identified as a protein binding to formin, a protein that regulates the actin cytoskeleton (19). FBP17 is a member of the *Schizosaccharomyces pombe* Cdc15 homology (PCH) protein family (20) and contains an N-terminal extended FER-CIP4 homology (EFC) domain (also known as the FER-CIP4 homology and Bin-amphiphysin-Rvs (F-BAR) domain), protein kinase C-related kinase homology region 1 (HR1), and an SH3 domain (Fig. 1*E*). The EFC/F-BAR domain has membrane binding and deformation activities, and FBP17 is involved in endocytosis in transfected COS-7 cells (18, 21, 22).

To confirm that FBP17 directly interacts with WIP or WASP, we performed GST pull-down assays using a fusion protein of GST and the SH3 domain of FBP17 (GST-FBPSH3). Purified GST and the GST-FSH3 fusion protein were subjected to SDS-PAGE (Fig. 1*F*, *lanes 1* and *2*). The HEK293 transfected cells express the Myc- and FLAG-tagged proteins (Fig. 1*F*, *lanes 3–6*). The results from the GST pull-down assays were shown (Fig. 1*F*, *lanes 7–14*). Both WASP and WIP were pulled down by GST-FSH3 (Fig. 1, *lanes 10* and *14*), indicating that the SH3 domain of FBP17 directly interacts with both proteins.

It has previously been shown that FBP17 binds to N-WASP and dynamin in transfected cells (18, 21). We examined whether FBP17 binds to WASP, WIP, and dynamin-2 in macrophages. THP-1 (human monocyte cell line) cells closely resemble monocyte-derived macrophages when differentiated by stimulation with PMA (23) and form podosomes and phagocytic cups that are morphologically and functionally indistinguishable from those in primary macrophages (supplemental Fig. 1) (4, 16, 23). WASP was immunoprecipitated from the lysates of PMA-differentiated THP-1 cells with an anti-WASP monoclonal antibody (Fig. 1*G*, *lanes 2*, *5*, and *8*) followed by immunoblotting using antibodies to FBP17 (21), WASP, and WIP. Both WIP and FBP17 co-immunoprecipitated with WASP (Fig. 1*G*, *lanes 5* and *8*). FBP17 also co-immunoprecipitated with dynamin-2 (Fig. 1*G*, *lanes 14*). These results, taken together with the results in Fig. 1*F*, suggest that FBP17 binds to the WASP-WIP complex and dynamin-2 in macrophages.

We next used immunofluorescence to examine whether FBP17 localizes at podosomes and phagocytic cups because the WASP-WIP complex is an essential component of podosomes (4, 15) and phagocytic cups (16). THP-1 cells transfected with FLAG-tagged FBP17 (FLAG-FBP17) and differentiated by stimulation with PMA were stained with an anti-FLAG monoclonal antibody to visualize FBP17 and with phalloidin to visualize the F-actin in podosomes and phagocytic cups (Fig. 1, *H* and *I*, *left* and *middle panels*). Merged images revealed that both F-actin and FBP17 are present in podosomes and phagocytic cups (Fig. 1, *H* and *I*, *right panels*), indicating that FBP17 localizes at podosomes and phagocytic cups.

Importance of FBP17 in the Formation of Podosomes and Phagocytic Cups—To determine the importance of FBP17 in the formation of podosomes and phagocytic cups, we knocked down FBP17 in THP-1 cells with siRNAs. To confirm that the expression of FBP17 was knocked down in cells, we transfected THP-1 cells with siRNAs, prepared lysates from the total

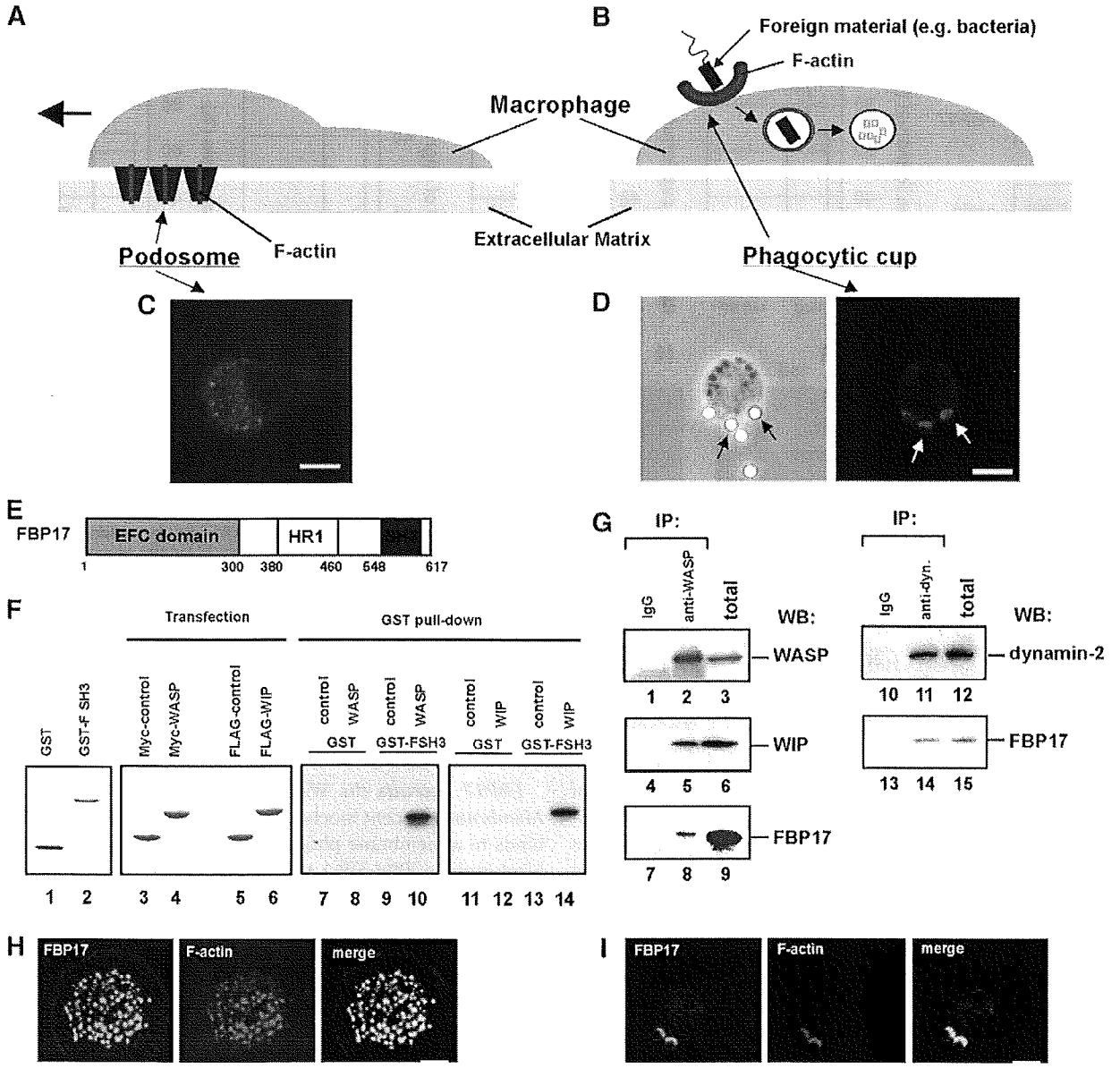

FIGURE 1. **FBP17 is a component of podosomes and phagocytic cups.** *A* and *B*, schematic drawings of podosomes (*A*) and a phagocytic cup (*B*) in macrophages. *C*, podosomes in macrophages were visualized by F-actin staining using Alexa Fluor 568-phalloidin. *D*, macrophages incubated with IgG-opsonized latex beads formed phagocytic cups to ingest the beads. A phase contrast image of a macrophage forming phagocytic cups (*left panel*). *Black arrows* indicate the latex beads ingested by the macrophage. Phagocytic cups were visualized by F-actin staining using Alexa Fluor 568-phalloidin (*right panel*). *White arrows* indicate the phagocytic cups.The *bar* is 10 μm. *E*, the domain organization of FBP17. *HR1*, protein kinase C-related kinase homology region 1. *F*, FBP17 interacts directly with WASP and WIP via its SH3 domain. GST and the GST-FBP17 SH3 domain fusion protein (GST-FSH3) were purified from bacteria extracts. Purified proteins were subjected to SDS-PAGEand stained with Coomassie Brilliant Blue (*lanes 1* and *2*). HEK293 cells were transfected with the cDNAs of Myc-tagged control protein (Myc-PDZ-GEF), Myc-WASP, FLAG-PDZ-GEF, or FLAG-WIP, and the expression of those proteins were analyzed by immunoblotting (*lanes 3–6*). Lysates from the HEK293 transfected cells were incubated with the affinity matrices of GST alone or GST-FSH3. Pull-down samples were analyzed by immunoblotting using anti-Myc antibody (*lanes 7–10*) and anti-FLAG antibody (*lanes 11–14*). *G*, FBP17 binds WASP, WIP, and dynamin-2. WASP was immunoprecipitated (*IP*) from the lysates of PMA-differentiated THP-1 cells with anti-WASP or a control IgG (*left panel, lanes 1–9*). The WASP immunoprecipitates and total lysates were analyzed by immunoblotting (*WB*) for WASP (*lanes 1–3*), WIP (*lanes 4–6*), and FBP17 (*lanes 7–9*). Dynamin was also immunoprecipitated from the THP-1 cell lysates with an anti-dynamin polyclonal antibody. The dynamin immunoprecipitates and total lysates were analyzed by immunoblotting for dynamin-2 (*lanes 10–12*) and FBP17 (*lanes 13–15*). *H* and *I*, confocal laser scanning micrographs of PMA-differentiated THP-1 cells. *H*, THP-1 cells transfected with FLAG-tagged FBP17 cDNA (FBP17) were double-stained with an anti-FLAG monoclonal antibody (*left panel*) and phalloidin (*center panel*) to visualize the F-actin in podosomes. *Yellow* indicates co-localization of FBP17 (*green*) and F-actin, podosomes (*red*) (*right panel*). *I*, THP-1 cells transfected with FLAG-FBP17 cDNA were incubated with IgG-opsonized latex beads and double-stained with anti-FLAG antibody and phalloidin. Phagocytic cups were visualized by F-actin staining (*center panel*). *Yellow* indicates co-localization of FBP17 (*green*) and F-actin, phagocytic cups (*red*) (*right panel*). The *bar* is 10 μm.

siRNAs-transfected cells, and analyzed the expression level of FBP17 by immunoblotting. THP-1 cells transfected with the siRNA for FBP17 expressed ~40% less FBP17 than cells transfected with a scrambled control siRNA based on the immunoblots (Fig. 2*A*, *lanes 1* and *2*) but expressed the same level of β-actin (Fig. 2*A*, *lanes 3* and *4*). The transfection efficiency of

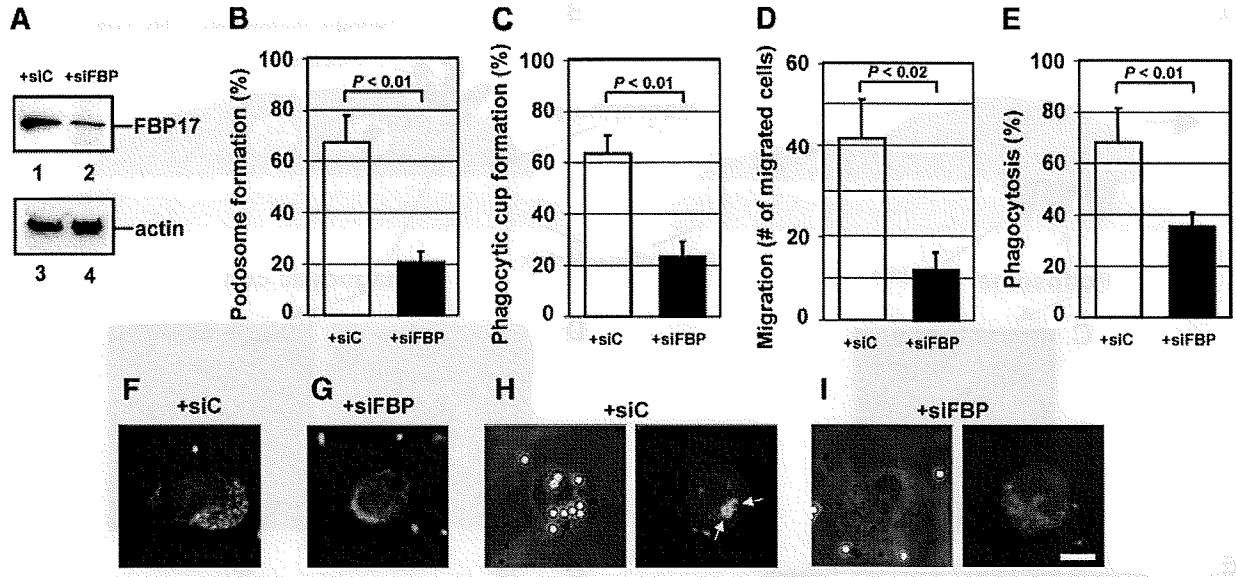

FIGURE 2. **The importance of FBP17 in the formation of podosomes and phagocytic cups.** *A*, expression of FBP17 was reduced by transfection of siRNA. THP-1 cells were transfected with siRNA for FBP17 (siFBP; *lanes 2* and *4*) or its scrambled control siRNA (siC; *lanes 1* and *3*). Lysates prepared from total transfected cells were analyzed by immunoblotting for FBP17 (*lanes 1* and *2*) and β-actin (*lanes 3* and *4*). *B* and *C*, effects of FBP17 siRNA on the formation of podosomes and phagocytic cups in macrophages. Human primary monocytes were co-transfected with siFBP (*closed bars*) or siC (*open bars*) and an FITC-conjugated control siRNA and then differentiated into macrophages with M-CSF-1. FITC-positive transfected cells were examined for the formation of podosomes (*B*) or phagocytic cups (*C*), and the percentage of cells with podosomes or phagocytic cups was scored. *D* and *E*, effects of FBP17 siRNA on the functions of podosomes and phagocytic cups. Macrophages co-transfected with siFBP (*closed bars*) or siC (*open bars*) and the FITC-conjugated control siRNA were assayed for macrophage migration (*D*) or phagocytosis of IgG-opsonized latex beads (*E*). Data represent the mean ± S.D. of triplicate experiments. *F–I*, immunofluorescence micrographs of a representative cell from each experiment. Cells transfected with siC (*F*) and siFBP (*G*) were stained with Alexa Fluor 568-phalloidin. Cells transfected with siC (*H*) or siFBP (*I*) were incubated with IgG-opsonized latex beads and then stained with phalloidin. The *left* and *right panels* are phase contrast and immunofluorescence micrographs, respectively. The *bar* is 10 μm.

THP-1 cells was estimated to be 40–50% from the expression of green fluorescent protein (GFP) used as a transfection control. Therefore, the decrease in FBP17 expression indicates that FBP17 was efficiently knocked down in most transfected cells.

Human primary monocytes were co-transfected with the FBP17 siRNAs and a FITC-conjugated control siRNA as a transfection marker. After differentiation of the monocytes into macrophages with M-CSF-1, FITC-positive cells were examined for the formation of podosomes and phagocytic cups. To quantify their formation, we scored the percentage of cells with podosomes or phagocytic cups among FITC-positive cells. When the expression of FBP17 was knocked down, the formation of both podosomes and phagocytic cups in macrophages was significantly reduced ($p < 0.01$; Fig. 2, *B* and *C*). These results suggest that FBP17 is necessary for the formation of podosomes and phagocytic cups. A representative cell from each experiment is shown in Fig. 2, *F* and *G*, for podosomes and in Fig. 2, *H* and *I*, for phagocytic cups. We then assayed macrophage migration as a podosome function and phagocytosis as a phagocytic cup function. When expression of FBP17 was knocked down, macrophage migration through a gelatin filter toward a chemoattractant was significantly reduced in cells transfected with FBP17 siRNA ($p < 0.02$; Fig. 2*D*). Phagocytosis of IgG-opsonized latex beads was also reduced (Fig. 2*E*). These results suggest that FBP17 is essential for chemotaxis and phagocytosis because of its role in forming podosomes and phagocytic cups, respectively.

FBP17 Recruits the WASP-WIP Complex to the Plasma Membrane—Recent biochemical analyses revealed that FBP17 binds to a membrane phospholipid, phosphatidylinositol 4,5-bisphosphate ($PI(4,5)P_2$), through its EFC/F-BAR domain and to N-WASP and dynamin via its SH3 domain (18, 21, 24). We have shown that although WASP and WIP are cytosolic proteins, the WASP-WIP complex localizes at podosomes and phagocytic cups (4, 16). We then examined whether FBP17 recruits the WASP-WIP complex to the plasma membrane in macrophages. We focused on the roles of the EFC and SH3 domains of FBP17 and constructed three FBP17 mutants for the recruitment experiments: a Lys-33 to Glu (K33E) substitution, a Lys-166 to Ala (K166A) substitution, and an SH3 domain deletion (dSH3). Both substitution mutations in the EFC domain (K33E and K166A) significantly reduce membrane binding and deformation (22), and the dSH3 mutant does not bind to WASP and WIP because the SH3 domain is the binding site of WASP and WIP (Fig. 1*F*). We co-transfected HEK293 cells with the FLAG-tagged FBP17 constructs, WASP, and WIP. A C-terminal fragment (1146–1429 amino acids) of PDZ-GDP exchange factor (PDZ-GEF) was used as a negative control for FBP17 because this fragment is stable in the cytosol and does not interact with any WASP-related proteins (4, 16, 25). We confirmed the expression of FBP17 and its mutants in cells by immunoblotting (supplemental Fig. 2) and immunoprecipitated FLAG-tagged proteins from lysates of the transfected cells with anti-FLAG antibody (Fig. 3*A*, *lanes 1–5*). WASP and WIP were detected in the immunoprecipitates from cells

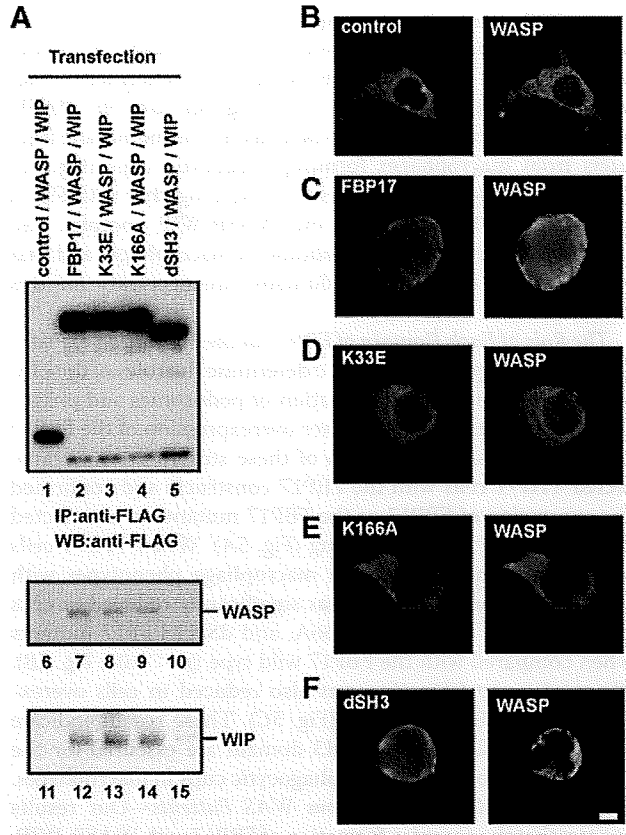

FIGURE 3. **FBP17 recruits WASP, WIP, and dynamin-2 to the plasma membrane.** *A*, HEK293 cells were co-transfected with cDNAs of the indicated FLAG-tagged proteins, Myc-tagged WASP, and HA-tagged WIP. The FLAG-tagged proteins were immunoprecipitated (*IP*) from lysates of the transfected cells with an anti-FLAG antibody followed by immunoblotting (*WB*) using antibodies to FLAG (*lanes 1–5*), WASP (*lanes 6–10*), and WIP (*lanes 11–15*). *B–F*, transfected HEK293 cells expressing FLAG-tagged proteins, Myc-WASP, and HA-WIP were double-stained with an anti-FLAG antibody and anti-WASP antibody. *B–F*, cells expressing FLAG-PDZ-GEF (*B*), FLAG-FBP17 (*C*), the FLAG-tagged FBP17 mutant with the K33E missense mutation (*D*), K166A (*E*), and the SH3-deleted FBP17 mutant dSH3 (*F*). The *bar* is 10 μm.

expressing the FLAG-tagged FBP17, K33E, and K166A constructs (Fig. 3*A*, *lanes 7–9* and *12–14*) but not the FLAG-tagged PDZ-GEF and dSH3 constructs (Fig. 3*A*, *lanes 6*, *10*, *11*, and *15*), indicating that FBP17 and its mutants K33E and K166A form a complex with WASP and WIP but that dSH3 not.

Next, cells expressing the FLAG-tagged proteins, WASP, and WIP were examined under the immunofluorescence microscope for the localization of the FLAG-tagged proteins and WASP. WASP and WIP were localized in the cytosol in cells transfected with only the WASP cDNA and only the WIP cDNA, respectively, as well as in cells expressing both WASP and WIP (supplemental Fig. 3). In cells co-expressing FLAG-PDZ-GEF (control) with WASP and WIP, both FLAG-PDZ-GEF and WASP were cytosolic (Fig. 3*B*). In cells co-expressing FLAG-FBP17 with WASP and WIP, FLAG-FBP17 localized at the plasma membrane because its EFC domain binds to the plasma membrane (Fig. 3*C*, *left panel*). In those cells, WASP also localized at the plasma membrane (Fig. 3*C*, *right panel*), indicating that FBP17 shifted the localization of WASP from the cytosol to the plasma membrane (Fig. 3, *B* and *C*). To confirm that the WASP-WIP complex was recruited to the plasma membrane, cells co-expressing FLAG-FBP17 with WASP and HA-tagged WIP were stained with an anti-FLAG monoclonal antibody and an anti-WASP polyclonal antibody or an anti-HA rat monoclonal antibody. Double staining revealed that both WASP and WIP co-localized with FLAG-FBP17 at the plasma membrane (supplemental Fig. 4, *A* and *B*). To further confirm the localization of the FBP17 mutants, cells co-expressing the FLAG-tagged FBP mutants, WASP, and WIP were stained with anti-FLAG monoclonal antibody. The K33E and K166A mutants were cytosolic and the SH3-deleted FBP17 mutant localized at the plasma membrane (supplemental Fig. 4*C*).

To determine the roles of the EFC and SH3 domains of FBP17 in this recruitment, we examined the localization of the FBP17 mutants and WASP in cells co-expressing the FBP mutants with WASP and WIP. Membrane tubulation in cells transfected with an FBP17 cDNA is an indicator of the membrane binding and deformation activities of FBP17 (18, 22). We detected *in vivo* membrane tubulation in cells expressing FBP17 and dSH3 but not in cells expressing K33E and K166A (supplemental Fig. 5). In cells co-expressing either FBP17 mutant (K33E or K166A) with WASP and WIP, both K33E and K166A were cytosolic (Fig. 3, *D* and *E*, *left panels*), and WASP was also cytosolic (Fig. 3, *D* and *E*, *right panels*). These results indicate that K33E and K166A are unable to recruit WASP to the plasma membrane, consistent with the inability of K33E and K166A to bind and deform the plasma membrane (supplemental Fig. 5).

The SH3-deleted FBP17 mutant, dSH3, localized at the plasma membrane (Fig. 3*F*, *left panel*) because its EFC domain is intact. However, WASP was cytosolic in cells co-expressing dSH3 with WASP and WIP (Fig. 3*F*, *right panel*), consistent with the inability of the dSH3 mutant to bind to WASP and WIP (Fig. 3*A*, *lanes 5*, *10*, and *15*).

To quantify the recruitment, we scored the percentage of cells in which WASP and WIP were localized at the plasma membrane. Cells expressing the FBP17 mutants (K33E, K166A, or dSH3) exhibited significantly lower plasma membrane localization of WASP and WIP than cells expressing FBP17 ($p < 0.05$; supplemental Fig. 6, *A* and *B*). FBP17 also recruited dynamin-2 to the plasma membrane, and both EFC and SH3 domains are necessary for this recruitment (supplemental Fig. 6*C*), as reported previously (18, 21). To confirm the localization of FBP17 and its mutants in cells co-expressing FBP17 with WASP, WIP, and dynamin-2, the transfected cells were stained with anti-FLAG monoclonal antibody. The wild-type FBP17 and dSH3 localized at the plasma membrane and the FLAG-PDZ-GEF (control) and the FBP mutants (K33E and K166A) were cytosolic (supplemental Fig. 6*D*).

Subcellular Localization of FBP17, WASP, WIP, and Dynamin-2 in Macrophages—To determine whether WASP, WIP, and dynamin-2 are recruited to the plasma membrane in macrophages when podosomes and phagocytic cups are formed, we examined the subcellular localization of FBP17, WASP, WIP, and dynamin-2 in macrophages forming podosomes or phagocytic cups. The cytosolic and membrane fractions were prepared from macrophages and analyzed by immunoblotting. Caspase-3 is a cytosolic marker, and sodium

potassium ATPase is a plasma membrane marker (26). FBP17 was detected in the membrane fraction from macrophages forming podosomes (Fig. 4*A*, *lane 9*). WASP, WIP, and dynamin-2 were also detected in the membrane fraction, although they are cytosolic proteins (Fig. 4*A*, *lanes 12*, *15*, and *18*). FBP17 was detected in the membrane fraction from macrophages forming phagocytic cups (Fig. 4*B*, *lane 9*). WASP, WIP, and dynamin-2 were also detected in the membrane fractions from macrophages forming phagocytic cups (Fig. 4*B*, *lanes 12*, *15*, and *18*). These results, taken together with Fig. 3, suggest that FBP17 recruits the WASP-WIP complex and dynamin-2 to the plasma membrane in macrophages and that both the EFC and the SH3 domains are necessary for this recruitment.

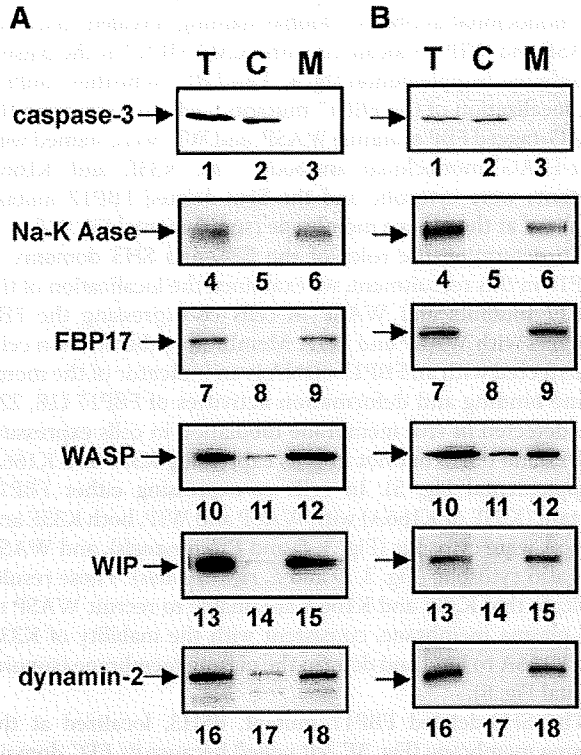

FIGURE 4. **Subcellular localization of FBP17, WASP, WIP, and dynamin-2 in macrophages.** *A*, macrophages forming podosomes. *B*, macrophages forming phagocytic cups. Total lysates (*T*), the cytosolic fraction (C), and the membrane fraction (*M*) prepared from macrophages forming podosomes (*A*) or phagocytic cups (*B*) were analyzed by immunoblotting for caspase-3 (*lanes 1–3*), sodium potassium ATPase (*Na-K Aase*; *lanes 4–6*), FBP17 (*lanes 7–9*), WASP (*lanes 10–12*), WIP (*lanes 13–15*), and dynamin-2 (*lanes 16–18*). Caspase-3 and sodium potassium ATPase (Na-K ATPase) are markers for the cytosol and plasma membrane, respectively.

The Role of Each Domain of FBP17 in the Formation of Podosomes and Phagocytic Cups—To determine the roles of the EFC and SH3 domains in the formation of podosomes and phagocytic cups, we examined whether overexpression of the FBP17 mutants affects the formation of these structures. We transfected THP-1 cells with the FBP17 constructs and confirmed the expression of FBP17 or the FBP17 mutants in transfected THP-1 cells by immunoblotting (Fig. 5*A*). When THP-1 cells were differentiated to obtain macrophage phenotypes with PMA, podosome formation was significantly reduced in cells overexpressing the K33E, K166A, and dSH3 FBP17 mutants when compared with the FBP17 wild type ($p < 0.01$; Fig. 5*B*). Phagocytic cup formation was also reduced in cells overexpressing the FBP17 mutants (Fig. 5*C*). These results indicate that the EFC domain and SH3 domain are essential for the formation of podosomes and phagocytic cups in macrophages.

Defects in Macrophages from WAS Patients—Our results suggest that the complex formation of FBP17 with WASP, WIP, and dynamin-2 at the plasma membrane is a critical step in the formation of podosomes and phagocytic cups (Figs. 1*G*, 3, and 4). In macrophages from WASP-deficient WAS patients, the complex does not form properly due to a lack of WASP expression. We examined macrophages from WASP-deficient WAS patients for the formation of podosomes and phagocytic cups. Two genetically independent WAS patients (WAS1, 211delT; and WAS2, 41–45delG) (27, 28) were assayed for the formation of those structures. Podosomes were completely absent (Fig. 6, *A–C*), and phagocytic cup formation was severely impaired (Fig. 6, *D–F*) in macrophages from both WAS patients, although FBP17, WIP, and dynamin-2 were expressed at the same level in patients as in normal individuals (Fig. 6*G*). In fact, the formation of podosomes and phagocytic cups was impaired in macrophages when the expression of WASP was reduced by siRNA transfection (4, 16). This is the first result showing that both podosome and phagocytic cup formations are defective in macrophages from WASP-deficient patients. These results are consistent with the previous observations (3, 12).

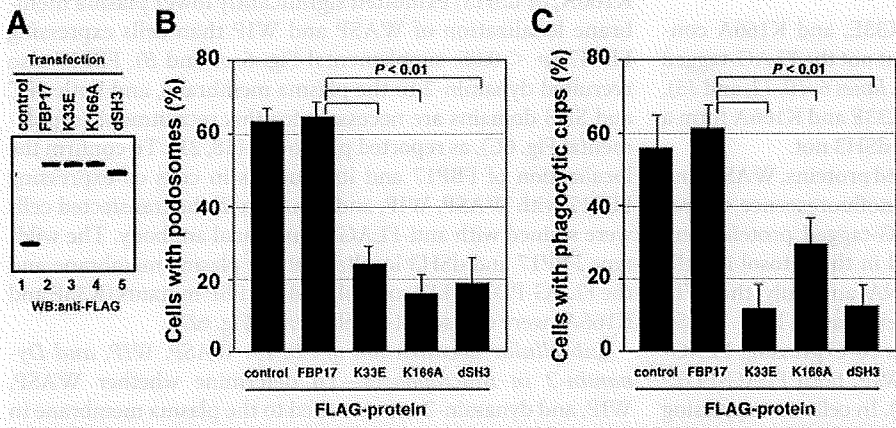

FIGURE 5. **The role of the EFC and SH3 domains of FBP17 in the formation of podosomes and phagocytic cups.** *A*, expression of FLAG-tagged proteins in transfected THP-1 cells. Total lysates prepared from transfected THP-1 cells were analyzed by immunoblotting (*WB*) using an anti-FLAG antibody. All of the FLAG-tagged proteins, FLAG-PDZ-GEF (control, *lane 1*), FLAG-FBP17 (*lane 2*), and the FBP17 mutants, K33E, K166A, and dSH3 (*lanes 3–5*) were expressed in THP-1 cells at similar levels. *B* and *C*, THP-1 cells co-transfected with cDNAs for the FLAG-tagged proteins and pmaxGFP were differentiated with PMA and then assayed for the formation of podosomes (*B*) and phagocytic cups (*C*). The percentage of cells with podosomes or phagocytic cups among all GFP-positive cells was scored. Data represent the mean ± S.D. of triplicate experiments.

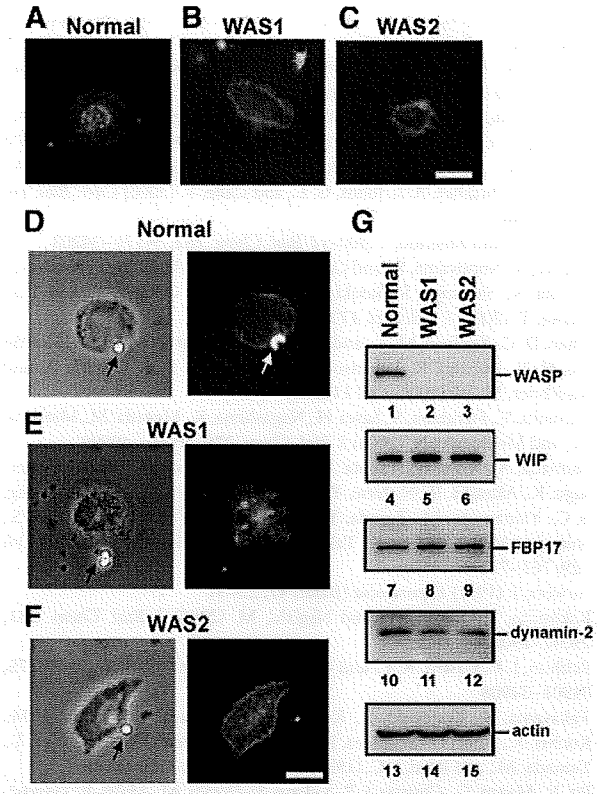

FIGURE 6. **Defective formation of podosomes and phagocytic cups in macrophages from WAS patients.** *A–F*, macrophages from a normal control and two genetically independent WAS patients (WAS1 and WAS2) were examined for the formation of podosomes (*A–C*) and phagocytic cups (*D–F*). The patients, WAS1 and WAS2, have the deletion mutations 211delT and 41–45delG, respectively, in their genomic DNAs. The *bars* are 10 μm. *G*, expression levels of WASP, WIP, FBP17, dynamin-2, and β-actin in WAS patients. Lysates prepared from macrophages from a normal control and two WAS patients (WAS1 and WAS2) were subjected to immunoblotting. WASP was not detected in the lysates from these WAS patients (*lanes 2* and *3*). Podosomes were completely absent (*A–C*) and phagocytic cup formation was severely impaired (*D–F*) in macrophages from both WAS patients, although FBP17, WIP, and dynamin-2 were expressed at the same level in patients as in normal individuals (*G*) (*lanes 4–12*).

These results give us a natural example that supports the importance of the complex formation of FBP17 with WASP, WIP, and dynamin-2 for the formation of podosomes and phagocytic cups.

DISCUSSION

Cell biological and structural analyses of the EFC domain of FBP17 have shown that the EFC domain binds to and deforms the plasma membrane (18, 22). It has previously been shown that the SH3 domain of FBP17 binds to N-WASP and dynamin in transfected cells (18, 21). However, physiologically important processes to which those activities of FBP17 contribute were unknown. Here, we have demonstrated that FBP17 recruits the WASP-WIP complex from the cytosol to the plasma membrane and that this recruitment is necessary for the formation of podosomes and phagocytic cups in macrophages. Our results suggest that FBP17 facilitates membrane deformation and actin polymerization induced by the WASP-WIP complex to occur simultaneously at the same membrane sites and that both are required for the formation of podosomes and phagocytic cups. This is supported by the observations that regulated actin polymerization is an essential process for the formation of podosomes (3) and phagocytic cups (29). Thus, FBP17 mediates a common molecular step in the formation of podosomes and phagocytic cups.

Macrophages have the ability to form both podosomes and phagocytic cups (Fig. 1, *A–D*). When macrophages having podosomes are stimulated with IgG-opsonized latex beads, the podosomes immediately disappear, and the phagocytic cups are formed at the site that the IgG beads attach. This observation indicates that the transition of the membrane structures occurs from podosomes to phagocytic cups. Macrophages migrate to sites of inflammation where they phagocytose pathogenic microbes and damaged tissue compounds and mediate local effector functions. Once macrophages encounter those materials at the site of inflammation, they stop migrating and phagocytose those materials. The transition of the macrophage functions occur from migration to phagocytosis. Podosomes and phagocytic cups are the essential membrane structures for migration and phagocytosis, respectively. Thus, the transition of the membrane structures from podosomes to phagocytic cups is essential and significant for the transition of the macrophage functions. Recently, two reports suggest that macrophage migration and phagocytosis include a common molecular mechanism to regulate actin cytoskeleton (40, 41). In this study, we identified a critical common molecular step mediated by FBP17 for the formation of podosomes and phagocytic cups, which are essential for migration and phagocytosis, respectively. In the future, elucidation of the molecular mechanisms underlying the transition would be intriguing.

It has been reported that dynamin-2 is also required for the formation of podosomes in transformed cells and osteoclasts (30–32) and phagocytic cups in a mouse macrophage cell line (33, 34) and that the FBP17-dynamin complex regulates the plasma membrane invagination (35). Our results suggest that FBP17 recruits dynamin-2 to the same site as membrane deformation and that this recruitment is also necessary for the formation of these structures (Figs. 3–5 and supplemental Fig. 6*C*). The formation of podosomes and phagocytic cups involves the process of the membrane protrusion (Fig. 1, *A–D*). The membrane protrusion requires the delivery of new membrane material (2). Our results, taken together with the above observations, suggest that dynamin-2 recruited by FBP17 to the plasma membrane probably plays an essential role in the formation of podosomes and phagocytic cups by regulating the recruitment of vesicles to the plasma membrane as new membrane material in macrophages.

Recently, the EFC domain of FBP17 was shown to bind strongly to the $PI(4,5)P_2$ (18, 22). On the other hand, it has been shown that $PI(4,5)P_2$ localizes at the podosomes in osteoclasts (36) and phagocytic cups (37, 38). These observations suggest that $PI(4,5)P_2$ is synthesized upon stimulation at the plasma membrane and plays an important role in the recruitment of FBP17 to the plasma membrane. Presumably, the $PI(4,5)P_2$ binding activity of the EFC domain is necessary for the localization of FBP17, and therefore, of the WASP-WIP complex and dynamin-2, at the sites where podosomes and phagocytic cups will form.

Role of FBP17 in the Podosome and Phagocytic Cup Formation

We suggest that the complex formation of FBP17 with WASP, WIP, and dynamin-2 at the plasma membrane is critical for the formation of podosomes and phagocytic cups (Figs. 1*G* and 3–5). In macrophages from WASP-deficient WAS patients, defects in the complex formation of FBP17 with WASP, WIP, and dynamin-2 impair the formation of podosomes and phagocytic cups (WAS1: 211delT (27); WAS2: 41–45delG(28) in Fig. 6), thereby reducing chemotaxis and phagocytosis by macrophages, which in turn would decrease the ability of host defense. The severity of WAS-associated symptoms was estimated and expressed as a score of 1–5. A score of 1 was assigned to patients with only thrombocytopenia and small platelets, and a score of 2 was assigned to patients with additional findings of mild, transient eczema or minor infections. Those with treatment-resistant eczema and recurrent infections despite optimal treatment received a score of 3 (mild WAS) or 4 (severe WAS). Regardless of the original score, if any patients then had autoimmune disease or malignancy, the score was changed to 5. The patients, WAS1 and WAS2, receive scores of 5 and 4, respectively. Both patients have the recurrent infections. We suggest that defective formation of podosomes and phagocytic cups in their macrophages (Fig. 6, *A–F*) reduces chemotaxis and phagocytosis, which are the critical processes to protect the body against infection, resulting in the recurrent infections. In addition, defective phagocytosis reduces the clearance of self-antigens such as apoptotic cells. This may cause the autoimmune diseases seen in WAS patients. In fact, Cohen *et al.* (39) recently reported that reduced clearance of apoptotic cells resulted in development of autoimmunity. Our findings therefore provide a potential mechanism for the recurrent infections and autoimmune diseases seen in WAS patients.

Acknowledgments—We thank Drs. M. Fukuda, R. C. Liddington, S. Courtneidge, A. Strongin (Burnham Institute for Medical Research), S. Grinstein (Hospital for Sich Children, Ontario, Canada), J. Condeelis (Albert Einstein Medical College), and P. De Camilli (Yale University) for critical reading of the manuscript and helpful discussion.

REFERENCES

1. Linder, S., and Aepfelbacher, M. (2003) *Trends Cell Biol.* **13,** 376–385
2. Linder, S. (2007) *Trends Cell Biol.* **17,** 107–117
3. Linder, S., Nelson, D., Weiss, M., and Aepfelbacher, M. (1999) *Proc. Natl. Acad. Sci. U. S. A.* **96,** 9648–9653
4. Tsuboi, S. (2007) *J. Immunol.* **178,** 2987–2995
5. Carman, C. V., Sage, P. T., Sciuto, T. E., Fuente, M. A. d. l., Geha, R. S., Ochs, H. D., Dvorak, H. F., Dvorak, A. M., and Springer, T. A. (2007) *Immunity* **26,** 784–797
6. Underhill, D. M., and Ozinsky, A. (2002) *Annu. Rev. Immunol.* **20,** 825–852
7. Leverrier, Y., and Ridley, A. J. (2001) *Curr. Biol.* **11,** 195–199
8. Wiskott, A. (1937) *Monatsschr. Kinderheilkd.* **68,** 212–216
9. Aldrich, R. A., Steinberg, A. G., and Campbell, D. C. (1954) *Pediatrics* **13,** 133–139
10. Notarangelo, L. D., Miao, C. H., and Ochs, H. D. (2008) *Curr. Opin. Hematol.* **15,** 30–36
11. Derry, J. M., Ochs, H. D., and Francke, U. (1994) *Cell* **78,** 635–644; Correction (1994) *Cell* **79,** 922
12. Lorenzi, R., Brickell, P. M., Katz, D. R., Kinnon, C., and Thrasher, A. J. (2000) *Blood* **95,** 2943–2946
13. Ramesh, N., Anton, I. M., Hartwig, J. H., and Geha, R. S. (1997) *Proc. Natl. Acad. Sci. U. S. A.* **94,** 14671–14676
14. Anton, I. M., de la Fuente, M. A., Sims, T. N., Freeman, S., Ramesh, N., Hartwig, J. H., Dustin, M. L., and Geha, R. S. (2002) *Immunity* **16,** 193–204
15. Chou, H. C., Anton, I. M., Holt, M. R., Curcio, C., Lanzardo, S., Worth, A., Burns, S., Thrasher, A. J., Jones, G. E., and Calle, Y. (2006) *Curr. Biol.* **16,** 2337–2344
16. Tsuboi, S., and Meerloo, J. (2007) *J. Biol. Chem.* **282,** 34194–34203
17. Tsuboi, S., Nonoyama, S., and Ochs, H. D. (2006) *EMBO Rep.* **7,** 506–511
18. Tsujita, K., Suetsugu, S., Sasaki, N., Furutani, M., Oikawa, T., and Takenawa, T. (2006) *J. Cell Biol.* **172,** 269–279
19. Chan, D. C., Bedford, M. T., and Leder, P. (1996) *EMBO J.* **15,** 1045–1054
20. Ho, H. Y., Rohatgi, R., Lebensohn, A. M., Le, M., Li, J., Gygi, S. P., and Kirschner, M. W. (2004) *Cell* **118,** 203–216
21. Kamioka, Y., Fukuhara, S., Sawa, H., Nagashima, K., Masuda, M., Matsuda, M., and Mochizuki, N. (2004) *J. Biol. Chem.* **279,** 40091–40099
22. Shimada, A., Niwa, H., Tsujita, K., Suetsugu, S., Nitta, K., Hanawa-Suetsugu, K., Akasaka, R., Nishino, Y., Toyama, M., Chen, L., Liu, Z. J., Wang, B. C., Yamamoto, M., Terada, T., Miyazawa, A., Tanaka, A., Sugano, S., Shirouzu, M., Nagayama, K., Takenawa, T., and Yokoyama, S. (2007) *Cell* **129,** 761–772
23. Auwerx, J. (1991) *Experientia (Basel)* **47,** 22–31
24. Kakimoto, T., Katoh, H., and Negishi, M. (2006) *J. Biol. Chem.* **281,** 29042–29053
25. Rebhun, J. F., Castro, A. F., and Quilliam, L. A. (2000) *J. Biol. Chem.* **275,** 34901–34908
26. Takayama, S., Krajewski, S., Krajewska, M., Kitada, S., Zapata, J. M., Kochel, K., Knee, D., Scudiero, D., Tudor, G., Miller, G. J., Miyashita, T., Yamada, M., and Reed, J. C. (1998) *Cancer Res.* **58,** 3116–3131
27. Jin, Y., Mazza, C., Christie, J. R., Giliani, S., Fiorini, M., Mella, P., Gandellini, F., Stewart, D. M., Zhu, Q., Nelson, D. L., Notarangelo, L. D., and Ochs, H. D. (2004) *Blood* **104,** 4010–4019
28. Imai, K., Morio, T., Zhu, Y., Jin, Y., Itoh, S., Kajiwara, M., Yata, J., Mizutani, S., Ochs, H. D., and Nonoyama, S. (2004) *Blood* **103,** 456–464
29. May, R. C., Caron, E., Hall, A., and Machesky, L. M. (2000) *Nat. Cell Biol.* **2,** 246–248
30. Ochoa, G. C., Slepnev, V. I., Neff, L., Ringstad, N., Takei, K., Daniell, L., Kim, W., Cao, H., McNiven, M., Baron, R., and De Camilli, P. (2000) *J. Cell Biol.* **150,** 377–389
31. McNiven, M. A., Baldassarre, M., and Buccione, R. (2004) *Front. Biosci.* **9,** 1944–1953
32. Bruzzaniti, A., Neff, L., Sanjay, A., Horne, W. C., De Camilli, P., and Baron, R. (2005) *Mol. Biol. Cell* **16,** 3301–3313
33. Gold, E. S., Underhill, D. M., Morrissette, N. S., Guo, J., McNiven, M. A., and Aderem, A. (1999) *J. Exp. Med.* **190,** 1849–1856
34. Tse, S. M., Furuya, W., Gold, E., Schreiber, A. D., Sandvig, K., Inman, R. D., and Grinstein, S. (2003) *J. Biol. Chem.* **278,** 3331–3338
35. Itoh, T., Erdmann, K. S., Roux, A., Habermann, B., Werner, H., and De Camilli, P. (2005) *Dev. Cell* **9,** 791–804
36. Chellaiah, M. A. (2005) *J. Biol. Chem.* **280,** 32930–32943
37. Botelho, R. J., Teruel, M., Dierckman, R., Anderson, R., Wells, A., York, J. D., Meyer, T., and Grinstein, S. (2000) *J. Cell Biol.* **151,** 1353–1368
38. Dewitt, S., Tian, W., and Hallett, M. B. (2006) *J. Cell Sci.* **119,** 443–451
39. Cohen, P. L., Caricchio, R., Abraham, V., Camenisch, T. D., Jennette, J. C., Roubey, R. A., Earp, H. S., Matsushima, G., and Reap, E. A. (2002) *J. Exp. Med.* **196,** 135–140
40. Brandt, D. T., Marion, S., Griffiths, G., Watanabe, T., Kaibuchi, K., and Grosse, R. (2007) *J. Cell Biol.* **178,** 193–200
41. Kato, M., Khan, S., d'Aniello, E., McDonald, K. J., and Hart, D. N. J. (2007) *J. Immunol.* **179,** 6052–6063
42. Calle, Y., Anton, I. M., Thrasher, A. J., and Jones, G. E. (2008) *J. Microsc. (Oxf.)* **231,** 494–505

Primary immunodeficiencies: 2009 update

International Union of Immunological Societies Expert Committee on Primary Immunodeficiencies: Luigi D. Notarangelo, MD,[a] Alain Fischer, MD,[b] and Raif S. Geha, MD[a] (Cochairs): Jean-Laurent Casanova, MD,[c] Helen Chapel, MD,[d] Mary Ellen Conley, MD,[e] Charlotte Cunningham-Rundles, MD, PhD,[f] Amos Etzioni, MD,[g] Lennart Hammartröm, MD,[h] Shigeaki Nonoyama, MD,[i] Hans D. Ochs, MD,[j] Jennifer Puck, MD,[k] Chaim Roifman, MD,[l] Reinhard Seger, MD,[m] and Josiah Wedgwood, MD, PhD[n] *Boston, Mass, Paris, France, New York, NY, Oxford, United Kingdom, Memphis, Tenn, Haifa, Israel, Stockholm, Sweden, Tokorozawa, Japan, Seattle, Wash, San Francisco, Calif, Toronto, Ontario, Canada, Zurich, Switzerland, and Bethesda, Md*

More than 50 years after Ogdeon Bruton's discovery of congenital agammaglobulinemia, human primary immunodeficiencies (PIDs) continue to unravel novel molecular and cellular mechanisms that govern development and function of the human immune system. This report provides the updated classification of PIDs that has been compiled by the International Union of Immunological Societies Expert Committee on Primary Immunodeficiencies after its biannual meeting in Dublin, Ireland, in June 2009. Since the appearance of the last classification in 2007, novel forms of PID have been discovered, and additional pathophysiology mechanisms that account for PID in human beings have been unraveled. Careful analysis and prompt recognition of these disorders is essential to prompt effective forms of treatment and thus to improve survival and quality of life in patients affected with PIDs.
(J Allergy Clin Immunol 2009;124:1161-78.)

Key words: *Primary immunodeficiencies, T cells, B cells, severe combined immunodeficiency, predominantly antibody deficiencies, DNA repair defects, phagocytes, complement, immune dysregulation syndromes, innate immunity, autoinflammatory disorders*

Since 1970, a committee of experts in the field of primary immunodeficiencies (PIDs) has met every 2 years with the goal of classifying and defining these disorders. The most recent meeting, organized by the Experts Committee on Primary Immunodeficiencies of the International Union of Immunological Societies, with support from the Jeffrey Modell Foundation and the National Institute of Allergy and Infectious Diseases of the National Institutes of Health, took place in Dublin, Ireland, in June 2009. In addition to members of the expert committee, the meeting gathered more than 30 speakers and more than 200 participants from 6 continents. Recent discoveries on the molecular and cellular bases of PID and advances in the diagnosis and treatment of these disorders were discussed. At the end of the meeting, the International Union of Immunological Societies Expert Committee on Primary Immunodeficiencies met to update the classification of PIDs, presented in Tables I to VIII.

The general outline of the classification has remained substantially unchanged. Novel PIDs, whose molecular basis has been identified and reported in the last 2 years, have been added to the list. In Table I (Combined T and B–cell immunodeficiencies), coronin-1A deficiency (resulting in impaired thymic egress) has been added to the genetic defects causing $T^- B^+$ severe combined immunodeficiency (SCID). The first case of DNA-activated Protein Kinase catalytic subunit (DNA-PKcs) deficiency has also been reported and adds to the list of defects of nonhomologous end-joining resulting in $T^- B^-$ SCID. Among calcium flux defects, defects of Stromal Interaction Molecule 1 (STIM-1), a Ca^{++} sensor, have been reported in children with immunodeficiency, myopathy, and autoimmunity. Mutations of the gene encoding the dedicator of cytokinesis 8 protein have been shown to cause an autosomal-recessive combined immunodeficiency with hyper-IgE, also characterized by extensive cutaneous viral infections, severe atopy, and increased risk of cancer. Also in Table I, mutations of the adenylate kinase 2 gene have been shown to cause reticular dysgenesis, and mutations in DNA ligase IV (LIG4), adenosine deaminase (ADA), and γc have been added to the list of genetic defects that may cause Omenn syndrome.

In Table II (Predominantly antibody deficiencies), mutations in Transmembrane Activator and CAML Interactor (TACI) and in B

From [a]the Division of Immunology, Children's Hospital Boston and Department of Pediatrics, Harvard Medical School; [b]Hopital Necker Enfants Malades, Paris; [c]Rockefeller University, New York; [d]the Department of Clinical Immunology, Oxford Radcliffe Hospitals; [e]the University of Tennessee and St Jude Children's Research Hospital; [f]Mount Sinai School of Medicine, New York; [g]Meyer's Children Hospital, Rappaport Faculty of Medicine, Technion, Haifa; [h]the Division of Clinical Immunology, Karolinska University Hospital Huddinge, Stockholm; [i]the Department of Pediatrics, National Defense Medical College, Tokorozawa; [j]the Department of Pediatrics, University of Washington School of Medicine; [k]the Department of Pediatrics, University of California at San Francisco; [l]The Sick Children's Hospital, Toronto; [m]Universitäs Kinderklinik, Zurich; and [n]the National Institute of Allergy and Infectious Diseases, Bethesda.

The Dublin meeting was supported by the Jeffrey Modell Foundation and by National Institute of Allergy and Infectious Diseases grant R13-AI-066891. Preparation of this report was supported by National Institutes of Health grant AI-35714 to R.S.G. and L.D.N.

Disclosure of potential conflict of interest: J.-L. Casanova has consulted for Centocor. H. Chapel has received research support from Baxter Healthcare, Talecris, and Biotest. M. E. Conley has received research support from the National Institutes of Health. C. Cunningham-Rundles has received research support from Baxter Corp. A. Fischer has contracted for INSERM, the European Community, and the French National Research Agency. R. S. Geha has received research support from the National Institutes of Health and the March of Dimes. L. Hammartröm has received research support from the National Institutes of Health, the European Community, and the Swedish Research Council. H. D. Ochs is on advisory boards for Baxter and CSL Behring and has received research support from the Jeffrey Modell Foundation, the National Institutes of Health/National Institute of Allergy and Infectious Diseases, and Flebogamma. J. Puck has received research support from the National Institutes of Health, the Jeffrey Modell Foundation, and Baxter; is on committees for USID Net and the Immune Deficiency Foundation; and is a board member of the Immune Tolerance Institute. The rest of the authors have declared that they have no conflict of interest.

Received for publication September 26, 2009; accepted for publication October 7, 2009.

Reprint requests: Luigi D. Notarangelo, MD, or Raif S. Geha, MD, Division of Immunology, Children's Hospital, One Blackfan Circle, Boston, MA 02115. E-mail: luigi.notarangelo@childrens.harvard.edu, raif.geha@childrens.harvard.edu.

0091-6749/$00.00

Published by Elsevier, Inc. on behalf of the American Academy of Allergy, Asthma, & Immunology

doi:10.1016/j.jaci.2009.10.013

Abbreviations used
ADA: Adenosine deaminase
PID: Primary immunodeficiency
SCID: Severe combined immunodeficiency

cell activating factor (BAFF)-receptor have been added to the list of gene defects that may cause hypogammaglobulinemia. However, it should be noted that only few TACI mutations appear to be disease-causing. Furthermore, variability of clinical expression has been associated with the rare BAFF-receptor deficiency. Table III lists other well defined immunodeficiency syndromes. Post-Meiotic Segregation 2 (PMS2) deficiency and immunodeficiency with centromeric instability and facial anomalies syndrome have been added to the list of DNA repair defects, whereas Comel-Netherton syndrome is now included among the immune-osseous dysplasias, and hyper-IgE syndrome caused by dedicator of cytokinesis 8 (*DOCK8*) mutation has also been added. Interleukin-2 Inducible T cell Kinase (ITK) deficiency has been included among the molecular causes of lymphoproliferative syndrome in Table IV (Diseases of immune dysregulation). Also in Table IV, CD25 deficiency has been listed to reflect the occurrence of autoimmunity in this rare disorder. Progress in the molecular characterization of congenital neutropenia and other innate immunity defects has resulted in the inclusion of Glucose-6-phosphate Transporter 1 (*G6PT1*) and Glucose-6-phosphate catalytic subunit 3 (*G6PC3*) defects in Table V (Congenital defects of phagocyte number, function, or both) and of MyD88 deficiency (causing recurrent pyogenic bacterial infections) and of CARD9 deficiency (causing chronic mucocutaneous candidiasis) in Table VI (Defects in innate immunity). Tables V and VI also include 2 novel genetic defects that result in clinical phenotypes distinct from the classical definition of PIDs. In particular, mutations of the Colony Stimulating Factor 2 Receptor Alpha (*CSF2RA*) gene, encoding for GM-CSF receptor α, have been shown to cause primary alveolar proteinosis as a result of defective surfactant catabolism by alveolar macrophages (Table V). Mutations in Apoliprotein L 1 (*APOL1*) are associated with trypanosomiasis, as reported in Table VI. It can be anticipated that a growing number of defects in immune-related genes will be shown to be responsible for nonclassic forms of PIDs in the future. Along the same line, the spectrum of genetically defined autoinflammatory disorders (Table VII) has expanded to include NLR family pyrin domain-containing 12 (*NLRP12*) mutations (responsible for familial cold autoinflammatory syndrome) and Interleukin-1 receptor antagonist (*IL1RN*) defects (causing deficiency of the IL-1 receptor antagonist). Again, it is expected that a growing number of genetic defects will be identified in other inflammatory conditions. Finally, defects of ficolin 3 (which plays an important role in complement activation) have been shown to cause recurrent pyogenic infections in the lung (Table VIII).

Although the revised classification of PIDs is meant to assist with the identification, diagnosis, and treatment of patients with these conditions, it should not be used dogmatically. In particular, although the typical clinical and immunologic phenotype is reported for each PID, it has been increasingly recognized that the phenotypic spectrum of these disorders is wider than originally thought. This variability reflects both the effect of different mutations within PID-causing genes and the role of other genetic, epigenetic, and environmental factors in modifying the phenotype. For example, germline hypomorphic mutations or somatic mutations in SCID-related genes may result in atypical/leaky SCID or Omenn syndrome, with the latter associated with significant immunopathology. Furthermore, infections may also significantly modify the clinical and immunologic phenotype, even in patients who initially present with typical SCID. Thus, the phenotype associated with single-gene defects listed in the revised classification should by no means be considered absolute.

Finally, a new column has been added to the revised classification to illustrate the relative frequency of the various PID disorders. It should be noted that these frequency estimates are based on what has been reported in the literature because with few exceptions, no solid epidemiologic data exist that can be reliably used to define the incidence of PID disorders. Furthermore, the frequency of PIDs may vary in different countries. Certain populations (and especially, some restricted ethnic groups of geographical isolates) have a higher frequency of specific PID mutations because of a founder effect and genetic drift. For example, DNA cross-link repair protein 1C (*DCLRE1C*) (Artemis) and Z-associated protein of 70 kD (*ZAP70*) defects are significantly more common in Athabascan-speaking Native Americans and in members of the Mennonite Church, respectively, than in other populations. Similarly, MHC class II deficiency is more frequent in Northern Africa. The frequency of autosomal-recessive immunodeficiencies is higher among populations with a high consanguinity rate.

TABLE I. Combined T and B–cell immunodeficiencies

Disease	Circulating T cells	Circulating B cells	Serum immunoglobulin	Associated features/atypical presentation	Inheritance	Molecular defect/presumed pathogenesis	Relative frequency among PIDs†
1. T^-B^+ SCID*							
(a) γc Deficiency	Markedly decreased	Normal or increased	Decreased	Markedly decreased NK cells Leaky cases may present with low to normal T and/or NK cells	XL	Defect in γ chain of receptors for IL-2, IL-4, IL-7, IL-9, IL-15, IL-21	Rare
(b) JAK3 deficiency	Markedly decreased	Normal or increased	Decreased	Markedly decreased NK cells Leaky cases may present with variable T and/or NK cells	AR	Defect in Janus activating kinase 3	Very rare
(c) IL-7Rα deficiency	Markedly decreased	Normal or increased	Decreased	Normal NK cells	AR	Defect in IL-7 receptor α chain	Very rare
(d) CD45 deficiency	Markedly decreased	Normal	Decreased	Normal γ/δ T cells	AR	Defect in CD45	Extremely rare
(e) CD3δ/CD3ε /CD3ζ deficiency	Markedly decreased	Normal	Decreased	Normal NK cells No γ/δ T cells	AR	Defect in CD3δ CD3ε or CD3ζ chains of T-cell antigen receptor complex	Very rare
(f) Coronin-1A deficiency	Markedly decreased	Normal	Decreased	Detectable thymus	AR	Defective thymic egress of T cells and T-cell locomotion	Extremely rare
2. T^-B^- SCID*							
(a) RAG 1/2 deficiency	Markedly decreased	Markedly decreased	Decreased	Defective VDJ recombination May present with Omenn syndrome	AR	Defect of recombinase activating gene (RAG) 1 or 2	Rare
(b) DCLRE1C (Artemis) deficiency	Markedly decreased	Markedly decreased	Decreased	Defective VDJ recombination, radiation sensitivity May present with Omenn syndrome	AR	Defect in Artemis DNA recombinase-repair protein	Very rare
(c) DNA PKcs deficiency	Markedly decreased	Markedly decreased	Decreased	[widely studied *scid* mouse defect]	AR	Defect in DNAPKcs Recombinase repair protein	Extremely rare
(d) ADA deficiency	Absent from birth (null mutations) or progressive decrease	Absent from birth or progressive decrease	Progressive decrease	Costochondral junction flaring, neurologic features, hearing impairment, lung and liver manifestations Cases with partial ADA activity may have a delayed or milder presentation	AR	Absent ADA, elevated lymphotoxic metabolites (dATP, S-adenosyl homocysteine)	Rare
(e) Reticular dysgenesis	Markedly decreased	Decreased or normal	Decreased	Granulocytopenia, deafness	AR	Defective maturation of T, B, and myeloid cells (stem cell defect) Defect in mitochondrial adenylate kinase 2	Extremely rare
3. Omenn syndrome‡	Present; restricted heterogeneity	Normal or decreased	Decreased, except increased IgE	Erythroderma, eosinophilia, adenopathy, hepatosplenomegaly	AR (in most cases)	Hypomorphic mutations in RAG1/2 , Artemis, IL-7Rα, RMRP, ADA, DNA ligase IV, γc	Rare
4. DNA ligase IV deficiency	Decreased	Decreased	Decreased	Microcephaly, facial dysmorphisms, radiation sensitivity May present with Omenn syndrome or with a delayed clinical onset	AR	DNA ligase IV defect, impaired nonhomologous end joining (NHEJ)	Very rare

(Continued)

TABLE I. *(Continued)*

Disease	Circulating T cells	Circulating B cells	Serum immunoglobulin	Associated features/atypical presentation	Inheritance	Molecular defect/presumed pathogenesis	Relative frequency among PIDs†
5. Cernunnos deficiency	Decreased	Decreased	Decreased	Microcephaly, *in utero* growth retardation, radiation sensitivity	AR	Cernunnos defect, impaired NHEJ	Very rare
6. CD40 ligand deficiency	Normal	IgM^+ and IgD^+ B cells present, other isotypes absent	IgM increased or normal, other isotypes decreased	Neutropenia, thrombocytopenia; hemolytic anemia, biliary tract and liver disease, opportunistic infections	XL	Defects in CD40 ligand (CD40L) cause defective isotype switching and impaired dendritic cell signaling	Rare
7. CD40 deficiency	Normal	IgM^+ and IgD^+ B cells present, other isotypes absent	IgM increased or normal, other isotypes decreased	Neutropenia, gastrointestinal and liver/biliary tract disease, opportunistic infections	AR	Defects in CD40 cause defective isotype switching and impaired dendritic cell signaling	Extremely rare
8. Purine nucleoside phosphorylase deficiency	Progressive decrease	Normal	Normal or decreased	Autoimmune hemolytic anemia, neurological impairment	AR	Absent purine nucleoside phosphorylase deficiency, T-cell and neurologic defects from elevated toxic metabolites (eg, dGTP)	Very rare
9. CD3γ deficiency	Normal, but reduced TCR expression	Normal	Normal		AR	Defect in CD3 γ	Extremely rare
10. CD8 deficiency	Absent CD8, normal CD4 cells	Normal	Normal		AR	Defects of CD8 α chain	Extremely rare
11. ZAP-70 deficiency	Decreased CD8, normal CD4 cells	Normal	Normal		AR	Defects in ZAP-70 signaling kinase	Very rare
12. Ca^{++} channel deficiency	Normal counts, defective TCR-mediated activation	Normal counts	Normal	Autoimmunity, anhydrotic ectodermic dysplasia, nonprogressive myopathy	AR AR	Defect in Orai-1, a Ca^{++} channel component Defect in Stim-1, a Ca^{++} sensor	Extremely rare
13. MHC class I deficiency	Decreased CD8, normal CD4	Normal	Normal	Vasculitis	AR	Mutations in *TAP1*, *TAP2*, or *TAPBP* (tapasin) genes giving MHC class I deficiency	Very rare
14. MHC class II deficiency	Normal number, decreased CD4 cells	Normal	Normal or decreased		AR	Mutation in transcription factors for MHC class II proteins (*C2TA*, *RFX5*, *RFXAP*, *RFXANK* genes)	Rare
15. Winged helix deficiency (Nude)	Markedly decreased	Normal	Decreased	Alopecia, abnormal thymic epithelium, impaired T-cell maturation [widely studied nude mouse defect]	AR	Defects in forkhead box N1 transcription factor encoded by *FOXN1*, the gene mutated in nude mice	Extremely rare
16. CD25 deficiency	Normal to modestly decreased	Normal	Normal	Lymphoproliferation (lymphadenopathy, hepatosplenomegaly), autoimmunity (may resemble IPEX syndrome), impaired T-cell proliferation	AR	Defects in IL-2Rα chain	Extremely rare
17. STAT5b deficiency	Modestly decreased	Normal	Normal	Growth-hormone insensitive dwarfism, dysmorphic features, eczema, lymphocytic interstitial pneumonitis, autoimmunity	AR	Defects of STAT5b, impaired development and function of γδT cells, regulatory T and NK cells, impaired T-cell proliferation	Extremely rare
18. Itk deficiency	Modestly decreased	Normal	Normal or decreased		AR	EBV-associated lymphoproliferation	Extremely rare

(Continued)

TABLE I. *(Continued)*

Disease	Circulating T cells	Circulating B cells	Serum immunoglobulin	Associated features/atypical presentation	Inheritance	Molecular defect/presumed pathogenesis	Relative frequency among PIDs†
19. DOCK8 deficiency	Decreased	Decreased	Low IgM, increased IgE	Recurrent respiratory infections. Extensive cutaneous viral and bacterial (staphylococcal) infections, susceptibility to cancer, hypereosinophilia, severe atopy, low NK cells	AR	Defect in *DOCK8*	Very rare

ADA, Adenosine deaminase; *AR*, autosomal-recessive inheritance; *ATP*, adenosine triphosphate; *C2TA*, class II transactivator; *EBV*, Epstein-Barr virus; *FOXN1*, forkhead box N1; *GTP*, guanosine triphosphate; *IL* (interleukin); *JAK3*, Janus associated kinase 3; *NHEJ*, non homologous end joining; *RFX*, regulatory factor X; *RMRP*, RNA component of mitochondrial RNA processing endonuclease; *NK*, natural killer; *RAG*, Recombinase Activating Gene; *SCID*, severe combined immune deficiency; *STAT*, signal transducer and activator of transcription; *TAP*, transporter associated with antigen processing; *TCR*, T cell receptor; *XL*, X-linked inheritance;
*Atypical cases of SCID may present with T cells because of hypomorphic mutations or somatic mutations in T-cell precursors.
†Frequency may vary from region to region or even among communities, ie, Mennonite, Innuit, and so forth.
‡Some cases of Omenn syndrome remain genetically undefined.
****Some metabolic disorders such methylmalonic aciduria may present with profound lymphopenia in addition to their typical presenting features.

TABLE II. Predominantly antibody deficiencies

Disease	Serum immunoglobulin	Associated features	Inheritance	Genetic defects/presumed pathogenesis	Relative frequency among PIDs
1. Severe reduction in all serum immunoglobulin isotypes with profoundly decreased or absent B cells					
(a) Btk deficiency	All isotypes decreased	Severe bacterial infections; normal numbers of pro-B cells	XL	Mutations in *BTK*	Rare
(b) μ heavy chain deficiency	All isotypes decreased	Severe bacterial infections; normal numbers of pro-B cells	AR	Mutations in μ heavy chain	Very rare
(c) λ5 deficiency	All isotypes decreased	Severe bacterial infections; normal numbers of pro-B cells	AR	Mutations in *IGLL1* (λ5)	Extremely rare
(d) Igα deficiency	All isotypes decreased	Severe bacterial infections; normal numbers of pro-B cells	AR	Mutations in Igα	Extremely rare
(e) Igβ deficiency	All isotypes decreased	Severe bacterial infections normal numbers of pro-B cells	AR	Mutations in Igβ	Extremely rare
(f) BLNK deficiency	All isotypes decreased	Severe bacterial infections normal numbers of pro-B cells	AR	Mutations in *BLNK*	Extremely rare
(g) Thymoma with immunodeficiency	All isotypes decreased	Bacterial and opportunistic infections; autoimmunity	None	Unknown	Rare
2. Severe reduction in at least 2 serum immunoglobulin isotypes with normal or low numbers of B cells					

(Continued)

TABLE II. *(Continued)*

Disease	Serum immunoglobulin	Associated features	Inheritance	Genetic defects/presumed pathogenesis	Relative frequency among PIDs
(a) Common variable immunodeficiency disorders (CVIDs)*	Low IgG and IgA and/or IgM	Clinical phenotypes vary: most have recurrent bacterial infections, some have autoimmune, lymphoproliferative and/or granulomatous disease	Variable	Unknown	Relatively common
(b) ICOS deficiency	Low IgG and IgA and/or IgM	—	AR	Mutations in *ICOS*	Extremely rare
(c) CD19 deficiency	Low IgG, and IgA and/or IgM	—	AR	Mutations in *CD19*	Extremely rare
(d) TACI deficiency**	Low IgG and IgA and/or IgM	—	AD or AR or complex	Mutations in *TNFRSF13B* (TACI)	Very common
(e) BAFF receptor deficiency**	Low IgG and IgM	Variable clinical expression	AR	Mutations in *TNFRSF13C* (BAFF-R)	Extremely rare
3. Severe reduction in serum IgG and IgA with normal/elevated IgM and normal numbers of B cells					
(a) CD40L deficiency***	IgG and IgA decreased; IgM may be normal or increased; B cell numbers may be normal or increased	Opportunistic infections, neutropenia, autoimmune disease	XL	Mutations in *CD40L* (also called *TNFSF5* or *CD154*)	Rare
(b) CD40 deficiency***	Low IgG and IgA; normal or raised IgM	Opportunistic infections, neutropenia, autoimmune disease	AR	Mutations in *CD40* (also called *TNFRSF5*)	Extremely rare
(c) AID deficiency****	IgG and IgA decreased; IgM increased	Enlarged lymph nodes and germinal centers	AR	Mutations in *AICDA* gene	Very rare
(d) UNG deficiency****	IgG and IgA decreased; IgM increased	Enlarged lymph nodes and germinal centers	AR	Mutation in *UNG*	Extremely rare
4. Isotype or light chain deficiencies with normal numbers of B cells					
(a) Ig heavy chain mutations and deletions	One or more IgG and/or IgA subclasses as well as IgE may be absent	May be asymptomatic	AR	Mutation or chromosomal deletion at 14q32	Relatively common
(b) κ chain deficiency	All immunoglobulins have lambda light chain	Asymptomatic	AR	Mutation in κ constant gene	Extremely rare
(c) Isolated IgG subclass deficiency	Reduction in one or more IgG subclass	Usually asymptomatic; may have recurrent viral/ bacterial infections	Variable	Unknown	Relatively common
(d) IgA with IgG subclass deficiency	Reduced IgA with decrease in one or more IgG subclass;	Recurrent bacterial infections in majority	Variable	Unknown	Relatively common
(e) Selective IgA deficiency	IgA decreased/absent	Usually asymptomatic; may have recurrent infections with poor antibody responses to carbohydrate antigens; may have allergies or autoimmune disease A few cases progress to CVID, others coexist with CVID in the same family.	Variable	Unknown	Most common

(Continued)